Total Environment Microbiology 2 (2026) 100070

Contents lists available at ScienceDirect

Total Environment Microbiology

journal homepage: www.elsevier.com/locate/temicr

Role of atmospheric transport in alteration of wintertime airborne pathogenic microbial communities over Arctic: A case study over Ny-Ålesund

Md Abu Mushtaque [a], Damodararao Karri [b], Shuvashree Maity [c], Naveen Gandhi [b], Rohit Srivastava [d], Christoph Ritter [e], Marion Maturilli [e], Uma Das [f], Sanat Kumar Das [a,*]

[a] Department of Physical Sciences, Bose Institute, Kolkata, West Bengal, India
[b] Indian Institute of Tropical Meteorology, Ministry of Earth Sciences, Pune, India
[c] Indian Institute of Science Education and Research, Pune, India
[d] National Centre for Polar and Ocean Research, Ministry of Earth Sciences, Goa, India
[e] Alfred Wegener Institute for Polar and Marine Research, Postdam, Germany
[f] Indian Institute of Information Technology Kalyani, Kalyani, West Bengal, India

ARTICLE INFO

Keywords:
Arctic
Precipitation
Bacteria
Fungi
Aerobiology

ABSTRACT

Recent climate change has caused pristine Arctic winter atmosphere to experience a strong variation in ambient temperature, leading to significant alterations in polar wind patterns and thereby, perturbation in airborne microbial community. Present study focuses on investigating atmospheric transported microorganisms via wind and clouds, altering polar microbial diversity in polar dark winter nights at Ny-Ålesund, Svalbard (78.9° N, 11.9°E), as part of the first Indian winter-time Arctic expedition conducted from 19th January to 12th February 2024. Average wintertime Arctic airborne cell concentration is noticed to be $1.5 \pm 0.5 \times 10^4$ per m^3. During the study period, Ny-Ålesund experiences a change in locally observed winter wind patterns from northerly winds to southerly winds. Significantly distinct clusters of microbial diversity are noticed corresponding to polar-influenced northerly wind (PW), southerly wind (SW) and precipitation (AP) over Ny-Ålesund. Microorganisms are primarily transported to Arctic by clouds, which contribute approximately one-third of bacterial and fungal genera through precipitation. In contrast, majority of pathogenic microorganisms are transported by PW, which carries fourfold more bacteria and 1.5-fold higher fungal genera than SW. Notably, PW transports 1.5-fold higher pathogenic bacterial genera than SW and two-fold higher compared to clouds. Several potential human pathogenic bacterial and fungal genera like *Pseudomonas, Acinetobacter, Staphylococcus, Corynebacterium, Aspergillus, Penicillium, Trichosporon, and Phaeococcomyces* are dominant in Arctic atmosphere. As many of these genera are commonly associated with respiratory and skin infections, and their presence highlights the need for continued microbial monitoring and research to better understand potential emerging health concerns.

1. Introduction

Arctic is experiencing rapid environmental transformation driven by climate change, with temperatures rising at nearly four-times global mean, a phenomenon known as Arctic amplification (Jensen et al., 2022; Lenton et al., 2008; Rantanen et al., 2022). The rapid warming has led to a significant reduction in snow cover (Bokhorst et al., 2016), particularly influencing atmospheric circulations over the polar region (Francis and Skific, 2015; Sasgen et al., 2024). Despite the persistent cold conditions ranging from -40 °C in winter to 15 °C in summer, the Arctic atmosphere remains rich in mixed-phase clouds year-round (Achtert et al., 2020; Cho et al., 2021). These clouds are composed of both supercooled liquid droplets and ice crystals and participate in regulating polar climate by altering radiative heat balance (Šantl-Temkiv et al., 2019). Alteration in radiative heat balance, particularly trapping of outgoing longwave radiation, leads to warming of the lower atmosphere, which in turn accelerates the melting of ice sheets. The melting of ice sheets, originally formed through cloud-driven precipitation processes, releases diverse microorganisms into the Arctic environment (Malard et al., 2023). These microorganisms are entrained within snow

* Corresponding author.
E-mail address: sanat@jcbose.ac.in (S.K. Das).

https://doi.org/10.1016/j.temicr.2026.100070
Received 8 December 2025; Received in revised form 6 February 2026; Accepted 17 February 2026
Available online 24 February 2026

and ice layer and are liberated into surface water and the atmosphere as melting occurs, creating a pathway for microbial redistribution between cryospheric and atmospheric reservoirs (Hopwood et al., 2020). Microorganisms in the Arctic environment span a wide range of sizes, from ultra-small single cells (~0.04 μm^3) to larger cells with aerodynamic diameters exceeding 2 μm (Dvoretsky et al., 2022). Due to their comparatively large size (often ~1 μm or larger) and chemically heterogeneous surfaces, bacteria are considered excellent cloud condensation nuclei (CCN) (Péguilhan et al., 2023). In addition to CCN activity, many of these microorganisms possess specialised nucleation properties, such as ice-nucleating protein and surface macromolecules, which enable them to catalyse ice formation and support cloud formation in cold atmospheres, even at temperatures less than or equal to −15 °C (Šantl-Temkiv et al., 2019). Several microorganisms, such as *Pseudomonas, Xanthomonas, and Bacillus,* are reported to be involved in cloud formation, acting as CCN at a temperature of -15 °C in winter and 0 °C in summer (Bauer et al., 2003; Kourtev et al., 2011). However, some other microorganisms like *Sphingomonas, Rhodococcus, Acinetobacter,* and the fungal genus *Aspergillus,* have also been identified in clouds (Amato et al., 2005; Fuzzi et al., 1997).

Several microorganisms have been reported to possess specific features that help them survive in extremely cold polar environments. *Arthrobacter* species tolerate desiccation and nutrient starvation, making them well-adapted to cold, harsh environments (Kourtev et al., 2011). *Pseudomonas* species exhibit metabolic versatility, including the ability to utilise diverse carbonaceous sources, grow autotrophically, and secrete siderophores for trace metal acquisition (Cody and Gross, 1987). *Bacillus* species form highly resistant spores that protect them from UV radiation, desiccation, and chemical stress (Setlow, 2006; Vaïtilingom et al., 2012). These survival strategies support microbial persistence and potential metabolic activity during atmospheric transport until wet deposition via precipitation. Wet deposition through precipitation is widely recognised as the most efficient removal process, capable of removing a large proportion of airborne particles under many circumstances (Després et al., 2012). Transport of airborne particles, including microorganisms, into the Arctic is seasonally dependent, with long-range transport of aerosols from mid-latitude continental regions occurring in winter and becoming especially pronounced during spring owing to the Arctic haze phenomenon (Jensen et al., 2022; Shaw, 1995). In contrast, summer season is characterised by thermal stratification (atmospheric stability) of the lower atmosphere, which restricts such long-range transport (Bozem et al., 2019; Jensen et al., 2022; Lange et al., 2019; Stohl, 2006). Recent studies across the whole Arctic region reported the dominance of anthropogenic haze during wintertime and strong local emissions during the summer season (Schmale et al., 2022).

Detection of microbial genera with known pathogenic potential in Arctic air masses is of particular concern, suggesting a possible link between long-range atmospheric transport and public health. Several bacterial genera frequently reported in atmospheric studies include *Staphylococcus, Streptococcus*, and *Acinetobacter*, which encompass clinically important species such as *Staphylococcus aureus*, associated with skin and respiratory tract infections (Gherardi, 2023); *Streptococcus pneumoniae*, a major cause of pneumonia and meningitis (Loughran et al., 2019); and *Acinetobacter baumannii*, a notorious multidrug-resistant hospital-acquired pathogen (Dijkshoorn et al., 2007). In addition, bacterial genera such as *Corynebacterium, Cutibacterium*, and *Anaerococcus*, typically regarded as commensals of human skin and mucosal surfaces, can act as opportunistic pathogens, particularly in immunocompromised individuals (John et al., 2025; Mayslich et al., 2021). Similarly, several fungal genera, including *Candida, Cryptococcus*, and *Aspergillus,* are clinically significant. *Candida* species are common agents of mucosal and systemic candidiasis (Makled et al., 2024), *Cryptococcus neoformans* is a leading cause of life-threatening meningitis in immunocompromised populations (Chen et al., 2022), and *Aspergillus fumigatus* is widely recognised as a cause of invasive pulmonary aspergillosis (Elkhapery et al., 2025). The presence of such potentially pathogenic microorganisms in Arctic air masses is therefore of concern for researchers and personnel operating in remote Arctic regions, where medical infrastructure is limited, and any sustained exposure or transmission could pose serious health consequences.

Despite growing interest in Arctic airborne microorganisms, current understanding of their composition, abundance, variability, and pathogenicity during the extremely cold and dark polar night remains limited, highlighting the need for comprehensive investigations into their sources, survival strategies, and transport mechanisms and pathogenicity during polar nights.

To fulfil this knowledge gap, present study aims to investigate wintertime Arctic airborne microorganisms under influence of wind-driven transport and cloud-associated precipitation. Understanding the composition and diversity of airborne and cloud-associated microorganisms in winter is essential, as subsequent melting of snow and ice in summer can release these microbes into the polar atmosphere (Harding et al., 2011). Once released, these microorganisms may influence local ecosystems, potentially affecting Arctic biodiversity (Cavicchioli et al., 2019; Vincent, 2010) and human health (Malard et al., 2023). Present study quantifies the influence of meteorological and atmospheric changes on airborne Arctic microbial communities and identifies potential pathogenic microorganisms that affect human health. By integrating microbial community data with meteorological parameters and atmospheric transport analysis, this work provides novel insights into composition and diversity of airborne microorganisms in the rapidly changing Arctic atmosphere, highlighting their ecological, climatic, and potential human health implications.

2. Site description & meteorological synopsis

Wintertime Arctic airborne microbial and aerosol samples are collected during polar dark nights at Ny-Ålesund, Svalbard (78.9° N, 11.9°E, 50 m above mean sea level) from 19th January to 12th February 2024, as part of the first Indian wintertime Arctic expedition in 2024. Ny-Ålesund is located on the west coast of Spitsbergen, the largest island of the Svalbard Archipelago, one of the northernmost inhabited archipelagos in the Arctic (shown in inset, Fig. 1). Mainland Norway lies south of the Barents Sea, with continental Europe further south and the Russian mainland to the east-southeast. Ny-Ålesund is a small village dedicated solely to serving as an international centre for Arctic research. Air samples are collected at the rooftop of Gruvebadet Observatory, located in a remote area of Ny-Ålesund. Gruvebadet Observatory is a fossil-fueled vehicle-free atmospheric laboratory. Extreme cold and harsh weather greatly restrict outdoor human activity, and no animal activity is observed in the immediate vicinity of the sampling site; occasional sightings of reindeer and Arctic foxes at distant locations are unlikely to have influenced the collected samples. Consequently, the site provides an ideal location for investigating airborne microbial communities under minimal human and animal influence. Being a high-latitude region, Ny-Ålesund experiences a typical polar winter atmosphere.

Five-days air parcel back-trajectories are simulated using the Hybrid Single Particle Lagrangian Integrated Trajectory (HYSPLIT) model for each sampling day between sampling periods, shown in Fig. 1(a). Two distinct clusters of back-trajectories are observed: one originating from continental regions of Europe and Russia, and considered as southerly wind (SW), and another originating from the North polar region, spending most of its time there and considered as polar-influenced wind (PW). Based on air mass back trajectories, air samples are thereby categorised into two groups as southerly (SW) and polar-influenced wind (PW) samples. Air masses classified as polar-influenced northerly winds predominantly remained within the ≥80° N latitude circle for approximately 4– 5 days prior to reaching the sampling site, justifying their classification as polar-influenced rather than purely polar. The detailed information is given in Table 1. Three Arctic precipitation (AP) samples are also collected during the sampling period and included in the present

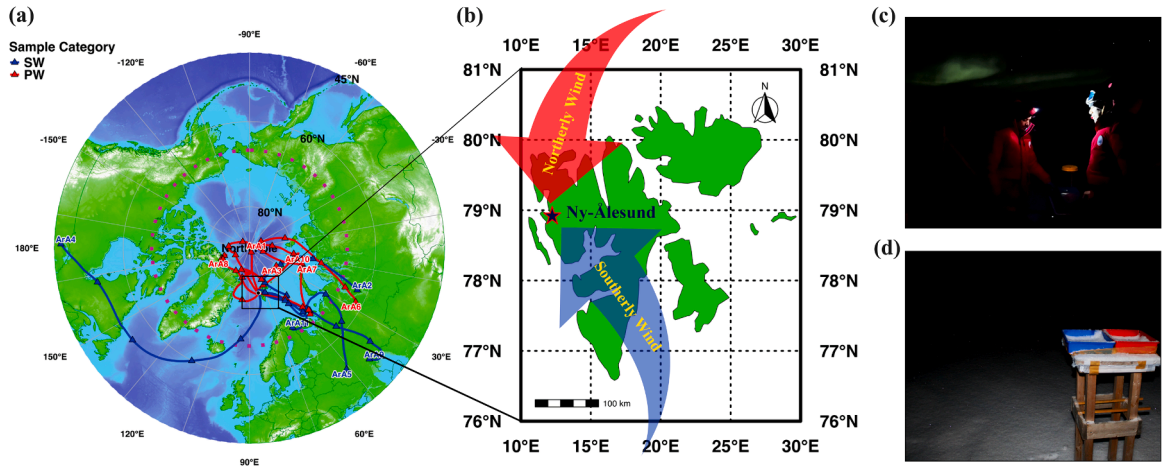

Fig. 1. (a) Geographical location of Ny-Ålesund with 5-day air parcel back-trajectories of each air sample collected during the sampling period. Triangles along the trajectory line indicate a 24-hour interval. (b) Location of Ny-Ålesund with arrows representing polar-influenced northerly wind (PW) and southerly winds (SW), (c) On-field picture of airborne sampling in polar nights, (d) Picture of on-field precipitation (snow) sample collection.

study.

Fig. 2 shows detailed information on meteorological conditions and vertical distribution of aerosol optical and physical properties over Ny-Ålesund. Each air sample, named ArA1 to ArA11, is collected for 48 h and is represented as horizontal grey bars in Fig. 2, while AP events are indicated by a symbol above horizontal grey bars. Meteorological data at one-minute intervals are obtained from the PANGAEA repository, and detailed measurement protocols are described in literature (Maturilli et al., 2013). During the sampling period at Ny-Ålesund, ambient air temperature (T) ranges from -20 °C to 6 °C, with occasional drops below -10 °C. The highest positive T of 6 °C is recorded on 26th January. Relative humidity (RH) varies between 40 % and 90 % throughout the sampling period, reaching a maximum on 25th January and a minimum on 22nd January. Wind direction (WD) is predominantly from the southeast and the north-northwest throughout the sampling period. Wind speed (WS) ranges from moderate to strong, with a peak value reaching up to 25 m/s on 23rd January. Notably, three precipitation samples are collected on 24th January, 31st January, and 01st February, respectively.

A continuous simultaneous measurement of aerosol vertical distribution is conducted using a ground-based lidar system operated by the Alfred Wegener Institute (AWI) in Ny-Ålesund from 19th January to 10th February. Hourly-averaged aerosol extinction coefficient (AE), depolarisation ratio (DR), and columnar aerosol optical depth (AOD) are also shown in Fig. 2. AE profiles reveal an aerosol layer extending up to 1.5 km, with a peak at 600 m above the ground. During SW period, AE near the surface (below 1 km) remained low with values around 5×10^{-3} m^{-1}, and on a few days (28th to 30th January) a distinct elevated layer between 1 and 2 km is noticed with higher values of $\sim 5 \times 10^{-2}$ m^{-1} and DR values between 0.1 and 0.2, suggesting the presence of spherical particles. In contrast, during PW, a separate aerosol layer is observed at a higher altitude between 2 and 3 km, with moderate AE ($\sim 1 \times 10^{-2}$ m^{-1}) and consistently high DR (0.5– 0.9), indicating non-spherical particles, likely ice crystals, sea salt or dust. Later, this elevated layer descended gradually, mostly coinciding with AP events (snowfall). AOD at 532 nm, the total area under the vertical profile of AE, exhibits substantial temporal variability, with background values typically ranging between 0.01 and 0.10 in Arctic polar nights. AOD is found to be 0.05 in SW and 0.10 in PW. Overall, lidar observations indicate that AOD is a factor of two higher in PW than in SW.

3. Methodology

3.1. Statistical analyses

In the present study, a Mantel test has been performed in order to evaluate the influence of various meteorological parameters (temperature (T), relative humidity (RH), wind speed (WS), and wind direction (WD)) and aerosol chemical compositions (Al, Si, Cr, Ni, Cu, Zn, As, Cd, Pb, NO_3^-, and SO_4^{2-}) on the overall structure of the whole airborne bacterial and fungal communities in the Arctic atmosphere. The Mantel test measures the correlation between two distance matrices. In the present study, the Mantel test compares a Bray-Curtis dissimilarity derived from microbial community composition with an Euclidean distance derived from individual environmental variables. Mantel test helps determine whether differences in environmental conditions correspond to changes in microbial community structure. The strength and direction of the correlation are indicated by Mantel's r, while Mantel's p-value reflects statistical significance. A significant result suggests that greater dissimilarity in an environmental variable is associated with increased dissimilarity in microbial communities. Principal component analysis (PCA) is an unconstrained multivariate ordination technique that reduces the dimensionality of complex datasets by transforming correlated variables into a smaller number of orthogonal principal components that explain the maximum variance in the data. In the present study, PCA is used to identify potential sources of air pollutants (metals and ions) by grouping elements or compounds with similar variance patterns. Canonical correspondence analysis (CCA) is a constrained ordination method that directly relates genus (OTU) abundance data to measured environmental variables. In this study, CCA is used to assess the influence of environmental parameters on bacterial and fungal OTU abundance at the genus level and identify key environmental drivers shaping microbial community composition. Principal coordinate analysis (PCoA) is a distance-based ordination technique that visualizes similarities and dissimilarities among samples using a chosen dissimilarity metric. In this study, PCoA is applied to examine variations in microbial community structure across different atmospheric conditions. PCoA are constructed depending on the Bray-Curtis similarity index calculated with OTU abundance data. PCoA is then applied with permutation multivariate analysis of variance (PERMANOVA) with 999 permutations to test for significant differences in microbial community structure among different atmospheric conditions. The Kruskal-Wallis test is used to assess significant differences in alpha diversity. The Kruskal–Wallis test is the nonparametric analog of a one-way ANOVA and does not assume normality. It is performed on the ranks of the

Table 1
Details of airborne sampling in wintertime Arctic atmosphere.

Sample	Date	Category	PM_{10}	Cell	T	Bacteria (V3-V4 region)						Fungi (ITS region)					
			($\mu g/m^3$)	(cell $/m^3$)	(°C)	Accession	Raw reads	Filtered reads	Shannon	Simpson	ChaoI	Accession	Raw reads	Filtered reads	Shannon	Simpson	ChaoI
ArA1	19/01–21/01	PW	30.98	1.5×10^4	-12.1	SAMN52588995	57,081	56,907	2.89	0.176	87	SAMN52627737	285,405	274,979	2.57	0.138	49
ArA2	21/01–23/01	SW	58.71	2.2×10^4	-3.8	SAMN52588996	71,708	71,517	3.52	0.060	77	SAMN52627738	2510,272	2386,519	2.53	0.257	778
ArA3	23/01–25/01	PW	77.38	1.2×10^4	-2.2	SAMN52588997	86,889	86,826	4.3	0.0217	119	SAMN52627739	322,689	311,622	2.85	0.074	42
ArA4	25/01–27/01	SW	111.48	1.9×10^4	1.4	SAMN52588998	71,823	71,525	4.02	0.026	85	SAMN52627740	255,326	246,653	2.32	0.149	40
ArA5	27/01–29/01	SW	45.26	2.2×10^4	-6.0	SAMN52588999	112,314	112,120	2.29	0.306	48	SAMN52627741	268,400	261,884	2.08	0.207	30
ArA6	29/01–31/01	PW	52.77	2.1×10^4	-6.1	SAMN52589000	85,110	84,923	3.12	0.118	74	SAMN52627742	479,757	463,192	1.65	0.28	38
ArA7	31/01–02/02	PW	36.13	9.7×10^3	-10.6	SAMN52589001	85,673	85,603	4.56	0.018	158	SAMN52627743	379,149	364,374	3.11	0.061	47
ArA8	02/02–04/02	PW	27.56	1.1×10^4	-7.1	SAMN52589002	70,639	70,439	3.15	0.088	60	SAMN52627744	156,060	151,185	2.51	0.125	36
ArA9	04/02–06/02	SW	15.29	7.4×10^3	-5.2	SAMN52589003	67,079	67,007	3.16	0.081	74	SAMN52627745	128,413	124,394	2.41	0.12	26
ArA10	06/02–08/02	PW	14.03	1.0×10^4	-9.5	SAMN52589004	88,699	88,699	3.95	0.047	125	SAMN52627746	113,761	113,303	4.9	0.391	1349
ArA11	08/02–10/02	SW	21.02	1.2×10^4	-8.2	SAMN52589005	84,094	84,026	3.53	0.060	90	SAMN52627747	159,075	157,228	2.68	0.095	39
ArP1	24/01/2024	AP	-	-		SAMN52589006	40,544	40,438	4.83	0.012	166	-	-	-	-	-	-
ArP2	31/01/2024	AP	-	-		SAMN52589007	32,293	32,211	4.13	0.037	114	SAMN52627748	324,826	317,350	2.75	0.115	88
ArP3	01/02/2024	AP	-	-		SAMN52589008	45,227	44,434	3.82	0.068	130	SAMN52627749	260,645	253,153	1.83	0.285	72

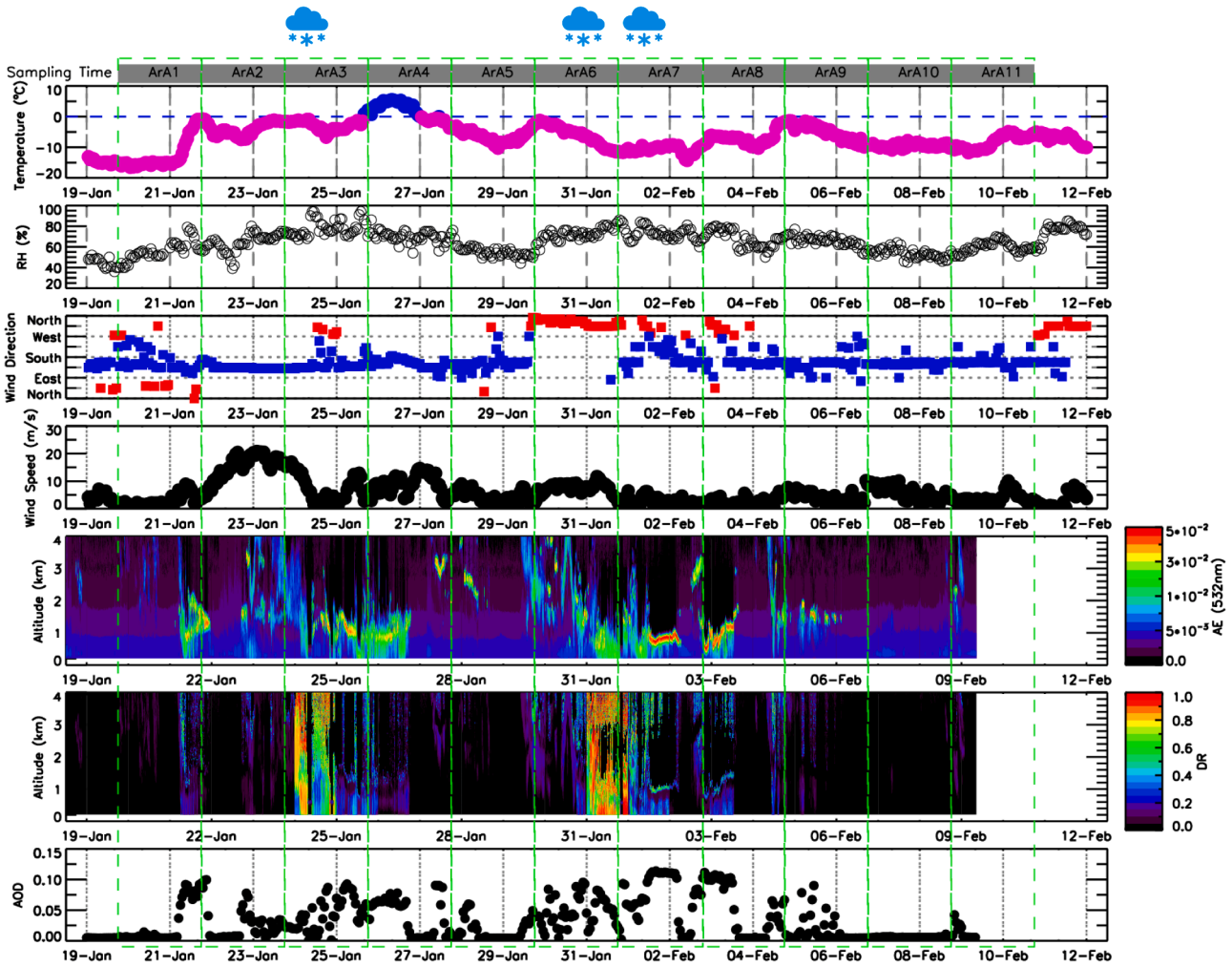

Fig. 2. Vertical green lines and horizontal grey bars at the top indicate the airborne sampling periods and the respective sample names, and a symbol above grey horizontal bars represents the precipitation periods. Temporal variation of key meteorological parameters during the observation period from 19th January to 12th February 2024, showing Air temperature (°C), Relative humidity (%), Wind direction, Wind speed, obtained from AWS, and vertical distribution of Aerosol extinction coefficient (AE), Aerosol depolarisation ratio (DR) and temporal variation of Aerosol optical depth (AOD), retrieved from Lidar observations.

measurement observations. Linear discriminant analysis effect size (LEfSe) identifies microbial genera that are significantly enriched across different atmospheric conditions by combining nonparametric statistical testing with linear discriminant analysis to estimate the effect size of differential features. Network analysis is employed to explore co-occurrence patterns among airborne microorganisms, allowing the identification of potential associations and interaction structures within microbial communities (Wang et al., 2024).

3.2. Sample collection

A total of 11 airborne microbial and aerosol samples are collected simultaneously at the sampling site throughout the Arctic expedition period for 48-hour intervals. Airborne microbial samples are collected with 4.7 cm radius mixed cellulose ester membrane filters with a pore size of 0.22 μm (Merck Life Science Private Limited, India) using an air vacuum pump. Aerosol samples are collected with quartz microfiber filters using a high-volume sampler (TISCH Environmental, USA) equipped with a PM_{10} impactor (Size Selective Inlet) and shown in Fig. 1 (c). The details of the airborne microbial sampling protocols are provided in the literature (Saikh et al., 2025; Saikh and Das, 2023), and for completeness, a brief description is provided below. After sampling, mixed cellulose ester membrane filters are transferred into cryovials containing 3 mL of TE (50 mM Tris, 50 mM EDTA [pH 7.8]). The cryovials are kept in a refrigerator for DNA sequencing. A quarter of each quartz microfiber filter is used to detect major ions (NO_3^- and SO_4^{2-}) using Ion Chromatography (IC) and trace metals (Al, Si, Cr, Ni, Cu, Zn, As, Cd, and Pb) using inductively coupled plasma mass spectroscopy (ICP-MS). The detail of the chemical analysis is provided in the literature (Pramanick et al., 2025).

Fresh AP samples are collected using a sterile tray placed 5 m above the ground to avoid any contamination from the ground (Fig. 1(d)). Prior to each sampling, the sampling tray is washed with autoclave Milli-Q water and sterilised with 70 % ethanol. AP samples are collected on 24th January, 31st January, and 01st February. Despite an AP event occurring on 26th January, samples could not be collected due to extreme weather conditions. Furthermore, samples collected on 21st January and 11th February are not included in the present study due to insufficient sample volume. After collection, AP samples are filtered using a mixed cellulose ester membrane filter, and subsequently processed using the same protocol as for airborne microbial sample filters. Airborne microbial and PM_{10} aerosol samples are collected simultaneously to ensure identical sampling durations and a special care has been taken to minimise potential human contamination during handling and filter exchange. Filter replacement is performed rapidly under aseptic conditions using sterile gloves and forceps to avoid any kind of contamination. Field blanks are also collected following the same handling and transport procedures to assess potential procedural

contamination. Blank samples are used solely for quality control and are excluded from the final dataset prior to analysis.

3.3. DNA extraction and high-throughput sequencing

DNA is isolated from the samples after cell suspension preparation using DNeasy PowerWater Kit (Qiagen), according to the manufacturer's protocol. To monitor potential contamination, a blank (negative control) is also processed in parallel through the same extraction procedure and further analysed alongside the bio-aerosol samples. DNA concentration is quantified spectrophotometrically using a Nano-Drop 2000 (Thermo). V3-V4 regions of the 16S rRNA gene are amplified from the metagenomic DNA using primers 341F (5′ CCTACGGGNGGCWGCAG 3′) and 785R (5′GACTACHVGGGTATC TAATCC 3′). Analogous primers are designed to amplify Internal Transcribed Spacer (ITS) region of small eukaryotes using ITS1F and ITS2R primers, respectively, in a nested PCR approach. Both positive and no-template controls are included in all PCR reactions. The PCR products are purified using AMPure XP beads (Beckman Coulter: 1X ratio) to remove non-specific fragments prior to library preparations. Final libraries are quantified using the 5300 fragment analyser system (Agilent). The validated libraries are sequenced on the Illumina NextSeq 2000 platform. After sequencing, two FASTQ files (forward and reverse) are generated for each sample, and adapter, barcodes, and primers are trimmed during initial quality control steps.

3.4. Sequence processing and analysis

Paired-end reads of raw sequences are merged using a minimum overlap length of 10 bp. Reads from the blank control sample are then mapped against the sample sequences using Bowtie2 in end-to-end, very-sensitive mode. Reads showing 100 % identity with the blank are removed from the sample data to eliminate potential contaminants. Following blank removal, the remaining sequences are filtered with the FastX-Toolkit (v0.0.12) using a minimum sequence length threshold of 100 bp and a minimum quality score of 20. High-quality reads are then clustered into operational taxonomic units (OTUs) at 97 % sequence similarity using the UPARSE pipeline. During OTU clustering, singletons and chimeric sequences are identified and discarded. Taxonomic assignment for each representative OTU is performed using the Ribosomal Database Project (RDP) classifier with a minimum confidence threshold of 80 %. The SILVA database is used for bacterial 16S rRNA gene sequences, and the UNITE database is used for fungal ITS sequences. Alpha diversity metrics, including Shannon and Simpson indices, are calculated using Perl scripts integrated within the UPARSE toolkit.

3.5. Cell count

Mixed cellulose ester membrane filters containing bioaerosols are cut into small pieces with sterile scissors within the cryovials under a laminar hood and vortexed continuously for 30 min to release microbial cells into the buffer. After vortexing, the mixture is allowed to stand for 2 to 3 min to let the filter fragments settle. The supernatant is then equally distributed into three sterile 1.5 mL centrifuge tubes and centrifuged at 2000 rpm for 5 s to pellet any remaining filter debris. The resulting supernatant is collected from all the tubes, and considered a suspension of microbial cells. 50 μL of cell suspension is transferred to a sterile 1.5 mL centrifuge tube and stained with 10 μg/mL 4′,6′ diamidino 2-phenylindole (DAPI) for 30 min in the dark at 40 °C. After staining, the cells are washed with sterile phosphate buffer saline (PBS) to remove excess dye. A 20 μL aliquot of stained suspension is then loaded into a hemocytometer and observed under a phase-contrast and a fluorescence microscope. The detailed procedure for total cell count is described in the literature (Saikh et al., 2025).

4. Results and discussion

4.1. Wintertime microbial airborne community

Atmospheric microbial cell (m^{-3}) and PM_{10} (μg/m^3) concentrations over Ny-Ålesund during sampling period are shown in Fig. 3 (a). Cell concentrations range from 7.4×10^3 to 2.2×10^4 cells/m^3 under SW, and from 9.7×10^3 to 2.2×10^4 cells/m^3 during PW conditions. Maximum cell concentration (2.2×10^4 cells/m^3) is measured in ArA2 and ArA5, whereas minimum cell concentration (7.4×10^3 cells/m^3) is observed in ArA9. Overall, microbial cell concentration observed over Ny-Ålesund is considerably lower than that reported from other regions. For Instance, higher concentrations of about $3.5 \pm 3 \times 10^6$ cells/m^3 and $6.7 \pm 1 \times 10^5$ cells/m^3 have been reported over high-altitude region of Namco, China (Tignat-Perrier et al., 2019) and Darjeeling, India (Pramanick et al., 2025), respectively. In contrast, markedly lower microbial cell concentrations of 7.2×10^2 cells/m^3 and 1.3×10^3 cells/m^3 have been reported over Southern Ocean (Malard et al., 2022) and Nuuk, Greenland (Šantl-Temkiv et al., 2018). PM_{10} concentrations are highest in ArA4 (111.5 μg/m^3) under SW while lowest concentration is observed in ArA10 (14.2 μg/m^3) during PW condition.

Culture-independent DNA amplicon sequencing of microbes collected from ambient air and precipitation samples yields 999 , 173 and 6 061 , 485 raw reads and 996 , 675 and 5 826 , 403 high-quality sequences after quality filtering for bacteria and fungi, respectively, that estimate 14 , 108 and 10 , 782 OTUs, and identify 1150 bacterial and 640 fungal genera at 97 % similarity.

Relative abundances of both bacterial and fungal genera present in all Arctic samples are shown in Fig. 3 (b) and (c). In PW samples, bacterial genera such as *Acinetobacter* (12.2 %), *Corynebacterium* (6.3 %), and *Staphylococcus* (6.2 %) are predominant, whereas in SW samples, *Hymenobacter* (8.4 %), *Acinetobacter* (8.2 %), and *Corynebacterium* (7.1 %) are predominant. Arctic precipitation is characterised by higher abundances of *Pseudomonas* (10.8 %), *Spirosoma* (10.1 %), and *Brevundimonas* (0.1 %). Among fungi, PW samples are dominated by *Aspergillus* (7.1 %), *Penicillium* (6.7 %), and *Candida* (4.6 %), while SW samples exhibit a higher proportion of *Aspergillus* (7.4 %), *Stemphylium* (7.2 %), and *Penicillium* (6.1 %). In precipitation, *Aspergillus* (6.7 %), *Cryptococcus_1* (4.7 %), *Penicillium* (3.4 %) and *Rhodotorula* (3.1 %) are most abundant. Notably, *Aspergillus* emerges as a consistently dominant fungal genus in both air and AP samples.

In the present study, the relative abundance of bacterial and fungal genera exhibits a strong variation due to changes in wind direction from polar-influenced northerly wind (PW) to southern wind (SW), as shown in Fig. 3 (c-d). In PW, *Acinetobacter* (21.1 %) has a maximum relative abundance in ArA6 sample followed by *Corynebacterium* in ArA1 (11.6 %) and ArA6 (10.8 %) samples. However, in SW, *Hymenobacter* has highest relative abundance (10.0 %) in ArA9 sample; *Blastocatella* (5.1 %) and *Geminicoccus* (5.2 %) are significantly present only in ArA5. *Penicillium* has the highest relative abundance of about 16.1 % in ArA1 followed by *Candida* with 11.4 % abundance noticed in ArA10 sample under PW conditions. In AP, bacterial genus *Pseudomonas* has maximum relative abundance (14.2 %) in AP2 sample, followed by *Spiromonas* (9.9 %) and *Brevundimonas*(9.0 %) in AP3, and *Hymenobacter* (7.1 %) in AP1, while fungal genus *Aspergillus* (7.8 %) has higher relative abundances, followed by *Cryptococcus_1* (5.8 %). Significant alterations in relative abundance of microbial genera are observed due to temporal and dynamic variations in North polar microbial communities. Similar variations are also reported in the relative abundance of the South Polar microbial community over Antarctica (Cao et al., 2021).

In the present study, dominant bacterial genera such as *Acinetobacter, Corynebacterium, Pseudomonas, Staphylococcus*, and fungal genera like *Aspergillus, Candida, Malassezia, Cryptococcus* are identified in both Arctic air and AP, which are reported as pathogenic microbes having potential cause for severe infections and diseases (Kourtev et al., 2011; Nemec et al., 2001; Wei et al., 2017; Zhu et al., 2018). The high

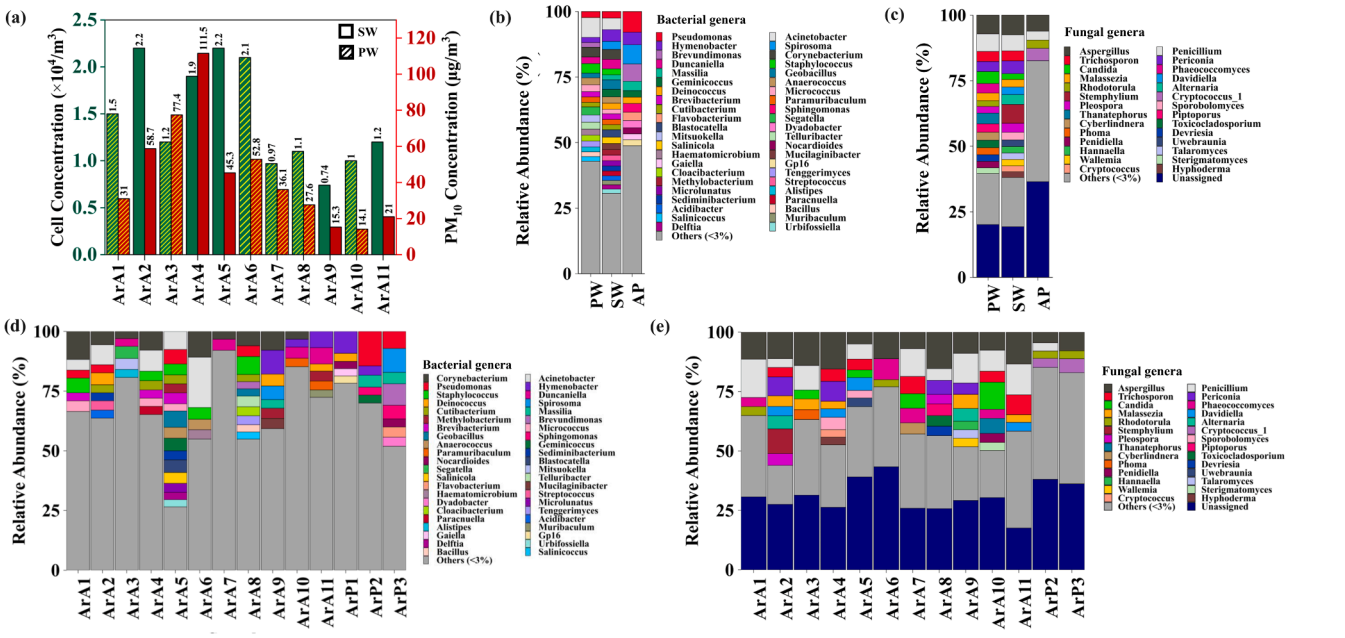

Fig. 3. (a) Number of total cell concentration and PM10 concentration in Arctic atmosphere, (b-c) Relative abundance of bacterial and fungal genera in polar wind (PW), southerly wind (SW), and precipitation (AP), (d-e) Relative abundance of bacterial and fungal genera in each sample.

abundance of microbes in the polar atmosphere in winter is due to their ability to be autotrophic, as well as to the production of siderophores to scavenge atmospheric transition metals as nutrients (Vaïtilingom et al., 2012). Interestingly, bacterial and fungal genera such as *Pseudomonas* and *Aspergillus,* dominant in Arctic AP samples, are also reported in clouds (Amato et al., 2005; Fuzzi et al., 1997), due to their involvement in cloud formation processes by acting as cloud condensation nuclei (CCN) and ice nuclei (IN) over Europe (Bauer et al., 2003; Kourtev et al., 2011).

4.2. *Biodiversity of microbial communities in different atmospheric conditions*

Average number of bacterial and fungal OTUs and genera of SW, PW, and AP are shown in Fig. 4 (a-b). AP contains more OTUs and genera in both bacterial and fungal communities. Interestingly, PW contains more genera than SW in both bacterial and fungal communities.

Arctic wintertime microbial alpha diversity has been studied using Shannon and Simpson indices, respectively, as shown in Fig. 4 (c-d). Bacterial Shannon diversity in AP (4.3 ± 0.5) is found to be higher than in the air. While in the air, PW contains relatively higher bacterial diversity (3.7 ± 0.7) than SW (3.3 ± 0.6). On the other hand, fungal diversity exhibits a reverse behaviour compared to bacterial diversity, with similar diversity values in SW (2.4 ± 0.2), PW (2.4 ± 0.6), and AP (2.3 ± 0.6).

Most of the dominant microbes present in AP have already been reported to act as CCN and IN particles (Amato et al., 2017; Fröhlich-Nowoisky et al., 2016; Šantl-Temkiv et al., 2019), participating in cloud formation; therefore, these microbes are considered cloud-borne microorganisms. Bacterial evenness (Simpson index) is minimum in AP (0.04 ± 0.03), followed by PW (0.08 ± 0.06), and high in SW (0.11 ± 0.11). However, fungal evenness is relatively higher in AP (0.20 ± 0.12) than in PW (0.13 ± 0.08) and SW (0.16 ± 0.06). The present study reveals that Arctic wintertime airborne bacterial population is highly diverse, with an evenly distributed pattern in air and clouds, whereas the Arctic fungi population has less variation, with an uneven distribution in both air and clouds. Cao et al. (2021) also reported that precipitation does not affect airborne bacterial diversity and evenness over Antarctica. A separate study over Greenland also reported that there is no significant difference between Arctic air and precipitation samples (Jensen et al., 2022). However, in the present study, Arctic winter PW contains significantly higher evenness than AP.

Beta diversity is further analysed using PCoA based on Bray-Curtis distance and shown in Fig. 4 (e-f). Bacterial ($p = 0.01$) and fungal ($p = 0.001$) communities contain three distinct groups of Arctic wintertime atmospheric microbial population. Airborne bacterial populations in SW and PW have little overlap, whereas cloud-borne microbes in AP form a separate cluster. Airborne fungal diversity exhibits distinguishably different clusters of PW and SW, as well as cloud-borne genera. Present study reveals a different airborne microbial community than that in cloud. Similarly, a distinct clusters of airborne bacteria representing different bacterial populations in air and precipitation are also reported in the Greenland Arctic (Jensen et al., 2022). Similar, distinct cluster of airborne bacteria in air and clouds are also reported elsewhere (Amato et al., 2017). Therefore, one can easily conclude that over polar region airborne bacteria have a different diversity than that in cloud.

4.3. *Bacterial and fungal genera in different atmospheric conditions*

Venn diagrams are employed to identify the unique cloud-borne microbes by considering simultaneous measurements of samples in air and AP over the sampling site, as shown in Fig. 5 (a-b). 159 unique bacteria (45 %) and 65 unique fungi (58 %) are identified as cloud-borne bacteria and fungi, respectively, and are considered for further analysis. It may be noted that almost 46 (12 %) bacterial and 30 (27 %) fungal genera are common, which could be mixed during AP. It is clearly showing that cloud carries more than twice as many bacteria as fungi over the sampling site. Fig. 5 (c-d) shows a Venn diagram for SW, PW, and AP. Analysis of bacterial genera reveals that the maximum number of unique bacteria is found in PW (30 %, 139), followed by cloud (28 %, 129), and the least in SW (8 %, 37). Similarly, the maximum number of unique fungal genera is found in cloud (31 %, 52), followed by PW (21 %, 36), and least in SW (15 %, 26). Notably, 2 % (10) of bacterial genera and 1 % (1) of fungal genera are common in all three conditions. The distinct distributions observed between bacterial and fungal genera highlight their differential responses to different environmental factors originating from the PW, SW, and in-cloud conditions. In SW, unique fungal genera (15 %) are found to be higher than those of unique

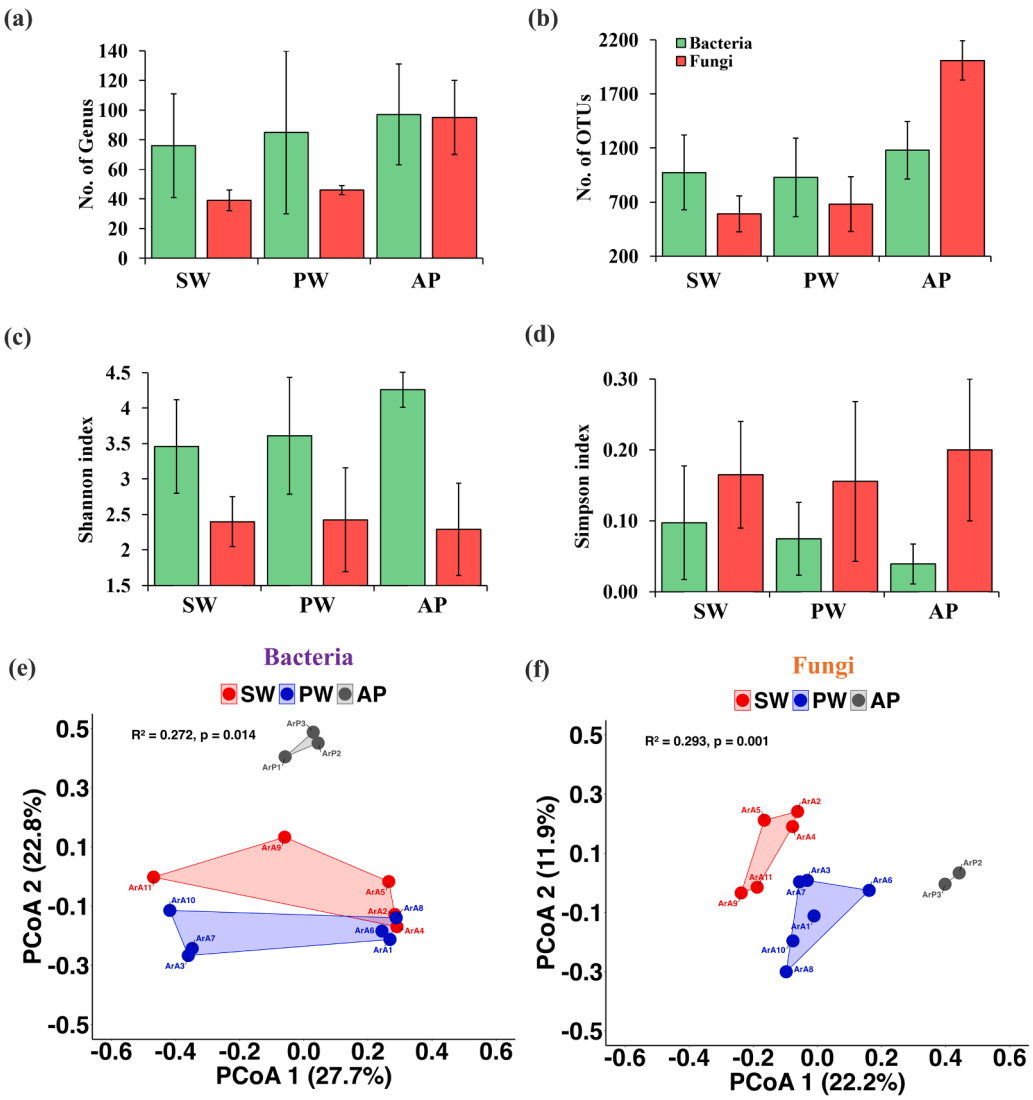

Fig. 4. (a) Number of bacterial and fungal operational taxonomic units (OTUs) in SW, PW, and AP, (b) Number of bacterial and fungal genera, (c) Shannon diversity index, (d) Simpson diversity index, (e-f) Beta diversity (PCoA) based on Bray-Curtis distance of bacterial communities and fungal communities.

bacterial genera (8 %). Common air bacteria are about 131, whereas common airborne fungi are about 43. However, PW wind has more unique airborne bacteria (139) than unique fungi (36), which could be due to the adaptability, transport, and survival mechanisms in the polar region that support maximum bacterial growth and proliferation (Doytchinov and Dimov, 2022).

Fig. 5 (e-f) illustrates the percentage contribution of bacterial and fungal genera to the Arctic atmosphere from various source categories. Common microbial genera detected in the air samples collected under both SW and PW conditions are classified as local and their sources are considered as 'local air'. This classification is based on their consistent presence irrespective of wind direction, indicating these genera are not influenced by changes in air-mass origin. In contrast, common genera detected in air samples associated with either SW and AP, PW and AP, or both SW and PW with AP are classified as 'mixed' reflecting contributions from both airborne and wet-deposition sources. A higher proportion of bacterial (28 %, 131) and fungal (25 %, 43) genera is found to be independent of wind origin, suggesting greater persistence of these genera in the local Arctic atmosphere. Only 6 % and 8 % of bacterial and fungal genera are found in the mixed sources. SW contributes 8 % and 15 % of the unique bacterial and fungal genera, respectively, to the Arctic atmosphere, while PW contributes 30 % and 21 % of these genera, respectively. Clouds through AP contribute 28 % and 31 % of bacterial and fungal genera, respectively, to the Arctic atmosphere, suggesting that clouds are the dominant microbial contributors to perturb Arctic wintertime microbial loading.

It is well documented in literature that the airborne microbial population shows a strong dependence on meteorological factors (Brągoszewska and Pastuszka, 2018; Saikh et al., 2025). In the present study, linear discriminant analysis effect size (LEfSe) is performed to distinguish indicator genera within SW, PW, and AP, with statistically significant differences. A total of 29 bacterial genera are distinguished using a default logarithmic LDA value of 2.5, as shown in Fig. 6. Consequently, 8, 7, and 14 representative bacterial genera are detected in SW, PW, and AP. Genera enriched in SW (*Streptococcus and Moraxella*) reflect contributions from terrestrial human-associated sources, supporting the hypothesis of ground-origin microbial input in SW (Velsko and Warinner, 2025). The presence of *Acinetobacter* and *Bacillus* in PW suggests the selection of psychrotolerant genera adapted to extreme polar environments (Nemec and Radolfova-Krizova, 2016). The enrichment of bacterial genera such as *Hymenobacter* and *Sphingomonas* in precipitation aligns with previous studies highlighting their atmospheric dispersal capabilities, survival at low substrate concentration, and resistance to UVs and oxidative stress (Eiler et al., 2003; Herrmann, 2003) which be due to survival within clouds over the polar region.

Similarly, a total of 24 fungal genera are significantly enriched using

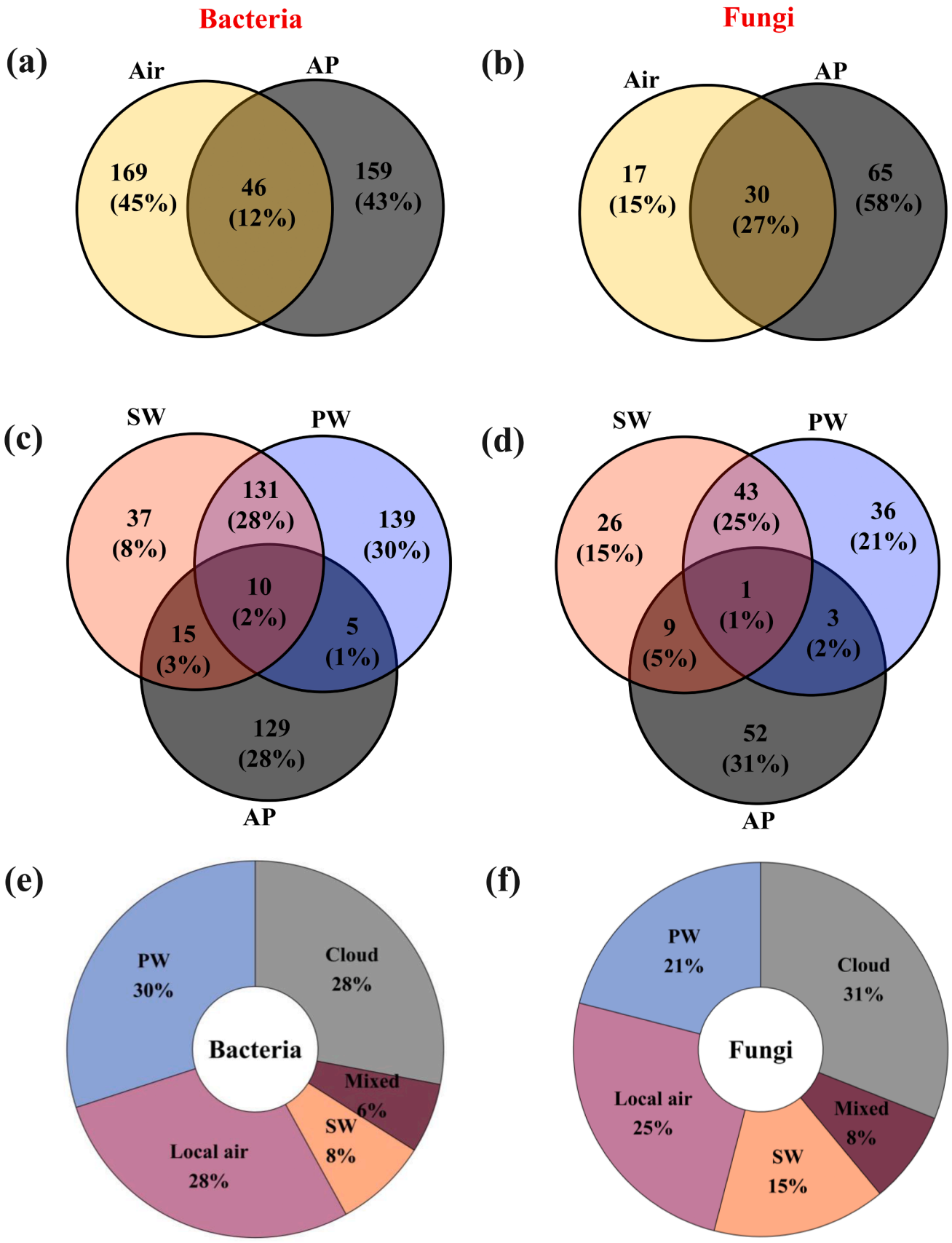

Fig. 5. Venn diagram illustrating common and unique bacterial and fungal genera in (a-b) simultaneous measurement of samples in air and precipitation, (c-d) SW, PW, and AP, (e-f) Pie chart illustrating the percentage of bacterial and fungal genera contributing to the Arctic atmosphere from various sources.

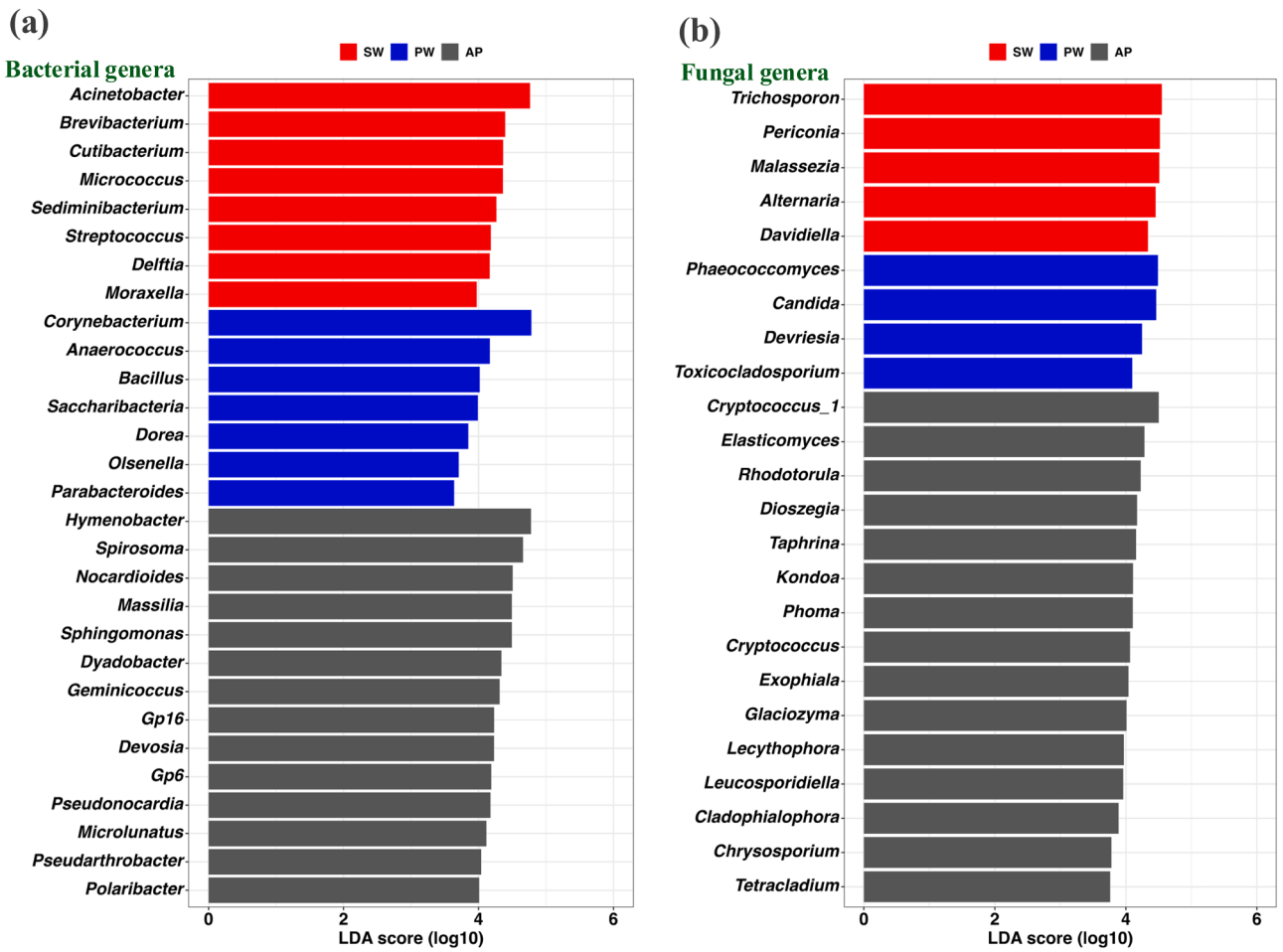

Fig. 6. Linear Discriminant Analysis Effect Size (LEfSe) result showing indicator (a) bacterial and (b) fungal genera within SW, PW, and AP with an LDA score (log10) greater than 2.5.

the default algorithmic LDA value of 2.5. Consequently, 5, 4, and 15 representative bacterial genera are detected in SW, WP, and AP. In the earlier studies, fungal genera such as *Cryptococcus, Rhodotorula*, and *Dioszegia* were also reported in colder environments (Butinar et al., 2007; Vaïtilingom et al., 2012). The dominance of *Cryptococcus_1, Rhodotorula*, and *Dioszegia* in precipitation reflects the presence of psychrotolerant and hydrophilic fungi capable of surviving within cloud droplets (Jarrige et al., 2022; Margesin et al., 2007; Zaragoza et al., 2009). Fungal genera enriched in PW, such as *Talaromyces* and *Devriesia*, are consistent with previous studies reporting their abundance in cold and nutrient-poor environments (Coutinho et al., 2019). In contrast, fungal genera such as *Candida, Alternaria*, and *Malassezia* in SW suggest strong terrestrial or anthropogenic influence, possibly from soil, plants, or human-associated sources (Blagojević et al., 2020; Gaitanis et al., 2012).

4.4. Metal concentration and source apportionment

In the present study, various types of major ions and metals present in the Arctic atmosphere during winter have been quantified, as detailed in Table 2. Among the major ions, SO_4^{2-} is found to be the most dominant with a mean concentration of 756 ± 489 μg/m^3, followed by NO_3^- at 160.4 ± 262 μg/m^3. Atmospheric SO_4^{2-} originates from both natural processes, such as mineral weathering, sea spray, and volcanic emissions, and anthropogenic activities such as coal combustion and industrial discharge. Similarly, NO_3^- is largely emitted from the oxidation of nitrogen oxides, originating from natural sources such as lightning, wildfires, and microbial processes, as well as from extensive anthropogenic sources such as vehicular emissions, agriculture, and industrial activities. Among the metals, Si, primarily associated with mineral dust, is most abundant, with a mean concentration of 3829.6 ± 1579 ng/m^3. Several heavy metals are also measured over Arctic atmosphere, with the mean concentration (in ng/m^3) arranged in decreasing order as follows: Zn (2079.9 ± 1043) > Cu (393.1 ± 180) > Pb (304.2 ± 263) > Al (111.4 ± 103) > Cr (13.5 ± 12) > Ni (12.0 ± 4) > As (3.8 ± 5) > Cd (2.3 ± 1). Airborne metals such as Cd, Ni, Cr, As, and Pb are known to be toxic and cause several health risks to humans, including dermatitis, osteoporosis, osteomalacia, kidney dysfunction, asthma, pneumonia, and various types of cancer (Mirzabeygi et al., 2017; Mushtaque et al., 2025; Sorahan and Esmen, 2004). These metals originate from various natural and anthropogenic sources. Atmospheric Al, Cr, As, and Pb commonly originate from both natural processes, such as rock weathering, volcanic activity, and anthropogenic activities like coal combustion, industrial emissions, mining, and waste incineration. Coal-fired power plants are particularly significant contributors, as coal contains trace levels of S, Pb, Cr, and As. These elements are emitted with stack gases and are known for their potential for long-range transport. While Al is less volatile, it is abundant in the mineral fraction of coal and is released as ash, making it a notable crustal and industrial tracer linked to coal combustion. Furthermore, studies have reported that wear and tear of brake linings, tires, and road surfaces release Cu, Zn, Ni, Cd, and Pb into the environment. For instance, brake pads are a significant source of Cu and Zn, while tires are a major contributor of Zn and Cd. Fuel combustion also contributes to Pb and Ni emissions. Both non-exhaust sources (brake, tire, and road wear) and exhaust (fuel

Table 2
Concentration of airborne major ions and heavy metals measured in wintertime Arctic atmosphere.

Sample	Date	Al ng/m^3	Si	Cr	Ni	Cu	Zn	As	Cd	Pb	NO_3^- µg/m^3	SO_4^{2-}
ArA1	19/01/2024–21/01/2024	70.2	5796.1	7.9	18.3	480.1	4326.4	2.8	2.8	145.5	79.8	463.1
ArA2	21/01/2024–23/01/2024	113.9	4987.3	2.5	15.4	481.8	3384.5	0.6	4.0	194.4	99.0	707.0
ArA3	23/01/2024–25/01/2024	84.1	4942.2	1.6	6.4	204.7	1537.7	0.4	2.4	81.2	60.6	324.7
ArA4	25/01/2024–27/01/2024	63.2	5816.4	5.9	7.2	178.7	1505.1	0.5	1.5	83.1	37.3	250.0
ArA5	27/01/2024–29/01/2024	50.9	3510.5	5.4	8.7	194.4	2056.4	0.8	1.6	103.2	49.2	348.0
ArA6	29/01/2024–31/01/2024	75.5	3387.3	11.3	11.7	321.3	1945.0	0.8	2.6	310.0	943.8	727.8
ArA7	31/01/2024–02/02/2024	77.0	2685.8	8.2	17.3	783.5	2937.8	1.2	3.8	909.1	120.9	1083.1
ArA8	02/02/2024–04/02/2024	82.4	2315.5	18.3	12.5	416.9	1731.2	6.9	2.2	303.0	120.4	683.7
ArA9	04/02/2024–06/02/2024	85.4	2092.6	14.8	9.0	294.8	1321.2	3.3	1.4	207.3	102.2	486.9
ArA10	06/02/2024–08/02/2024	417.8	1417.2	36.4	12.7	529.2	1079.3	10.3	1.8	677.1	37.7	1554.9
ArA11	08/02/2024–10/02/2024	104.7	5174.8	36.7	12.8	438.4	1054.0	13.9	1.6	332.4	113.3	1687.6
Overall Mean±std		111.4 ± 103	3829.6 ± 1579	13.5 ± 12	12.0 ± 4	393.1 ± 180	2079.9 ± 1043	3.8 ± 5	2.3 ± 1	304.2 ± 263	160.4 ± 262	756.1 ± 489
PW Mean±std		134.5 ± 138	3424.0 ± 1657	13.9 ± 12	13.1 ± 4.3	455.9 ± 198	2259.6 ± 1185	3.7 ± 4	2.6 ± 1	404.3 ± 322	227.2 ± 352	806.2 ± 449
SW Mean±std		83.6 ± 27	4316.3 ± 1502	13.1 ± 14	10.6 ± 3	317.6 ± 138	1864.2 ± 925	3.8 ± 5.8	2.0 ± 1	184.1 ± 99	80.2 ± 34	695.9 ± 580

combustion) sources contribute substantially to the metal content of urban air and road dust (Adamiec et al., 2016; Hawari et al., 2021).

To identify the dominant sources of atmospheric metals in the Arctic, principal component analysis (PCA) is performed. PCA analysis identifies three principal components (PCs), as mentioned in Table 3, which collectively explain 82 % of the total variance, with PC1, PC2, and PC3 accounting for 40.6 %, 30.4 %, and 11.2 %, respectively. Source attribution is based on elemental markers associated with each PC. PC1 exhibits high loading for Al, Cr, As, Pb, and SO_4^{2-}, indicating influence of industrial emissions (Altıkulaç et al., 2022; Huang et al., 2017; Labus, 1995; Munawer, 2018). PC2, with high loading for Ni, Cu, Zn, Cd, and Pb, reflects urban anthropogenic sources related to traffic emissions and fuel combustion (Adamiec et al., 2016; Hawari et al., 2021). PC3 is characterised by a high loading of NO_3^-, suggesting contributions from shipping activities, including emissions from ships/marine vessels, small boats, and other marine-related activities near the Arctic (Sonbawne et al., 2023). Due to the remoteness of the sampling site and the absence of significant local industrial and urban activities, the majority of the measured metals are attributed to long-range transport from distant sources, particularly the Eurasian region.

Table 3
Varimax rotated principal component analysis of metals present in Arctic atmosphere.

	PC1	PC2	PC3
Al	0.74	0.01	0.18
Si	-0.44	0.04	-0.73
Cr	0.96	-0.13	0.008
Ni	0.19	0.93	-0.07
Cu	0.42	0.87	0.15
Zn	-0.48	0.78	-0.24
As	0.92	-0.09	-0.21
Cd	-0.29	0.88	0.10
Pb	0.57	0.55	0.48
NO_3^-	-0.21	0.01	0.65
SO_4^{2-}	0.90	0.27	0.08
Variance (%)	40.6	30.4	11.2
Cumulative (%)	40.6	71.1	82.3
Eigenvalues	4.4	3.3	1.2

4.5. Relation between environmental variables and microbial communities

In the present study, a Mantel test has been performed in order to evaluate the influence of various meteorological parameters (temperature (T), relative humidity (RH), wind speed (WS), and wind direction (WD)) and aerosol chemical compositions (Al, Si, Cr, Ni, Cu, Zn, As, Cd, Pb, NO_3^-, SO_4^{2-}) on the overall structure of the whole airborne bacterial and fungal communities in the Arctic atmosphere (Fig. 7 (a)). Analysis reveals that the whole bacterial community structure is strongly influenced by Cr, Ni, Cu, and SO_4^{2-} whereas major ions such as NO_3^- and SO_4^{2-} and meteorological parameters including T, WD, and RH strongly influence whole fungal communities. However, only Cr ($p < 0.05$), As ($p < 0.05$) and SO_4^{2-} ($p < 0.05$) exhibit statistically significant influence on the whole bacterial community. In contrast, among the meteorological parameters, only WD ($p < 0.05$) significantly influences the whole fungal community. In addition, Spearman correlation among metals exhibit a significant positive correlation between As and Cr ($p < 0.001$), Cr and Al ($p < 0.05$), Al and SO_4^{2-} ($p < 0.05$), SO_4^{2-} and Pb ($p < 0.05$), SO_4^{2-} and As ($p < 0.01$). These relationships suggest a common industrial or combustion source. Similarly, Cd exhibit significant positive correlations with Ni ($p < 0.05$), Cu ($p < 0.05$), and Zn ($p < 0.01$), while Pb correlated positively with Cu ($p < 0.001$), Cu with Ni ($p < 0.001$), and Ni with Zn ($p < 0.05$), further supporting a common origin, as also indicated by the PCA results.

To further investigate the impact of environmental factors on specific bacterial and fungal genera, Canonical Correspondence Analysis (CCA) is performed using the full set of meteorological and chemical composition data (Fig. 7 (b-c)). CCA results indicate that bacterial genera such as *Moraxella, Sediminibacterium, Micrococcus, Brevibacterium, and Cutibacterium* which are enriched under SW conditions are positively associated with Zn, Si, and Ni, typically emitted from urban traffic sources. Spearman correlation analysis supports these associations, showing significant correlation between Zn and Si and *Moraxella, Delftia, and*

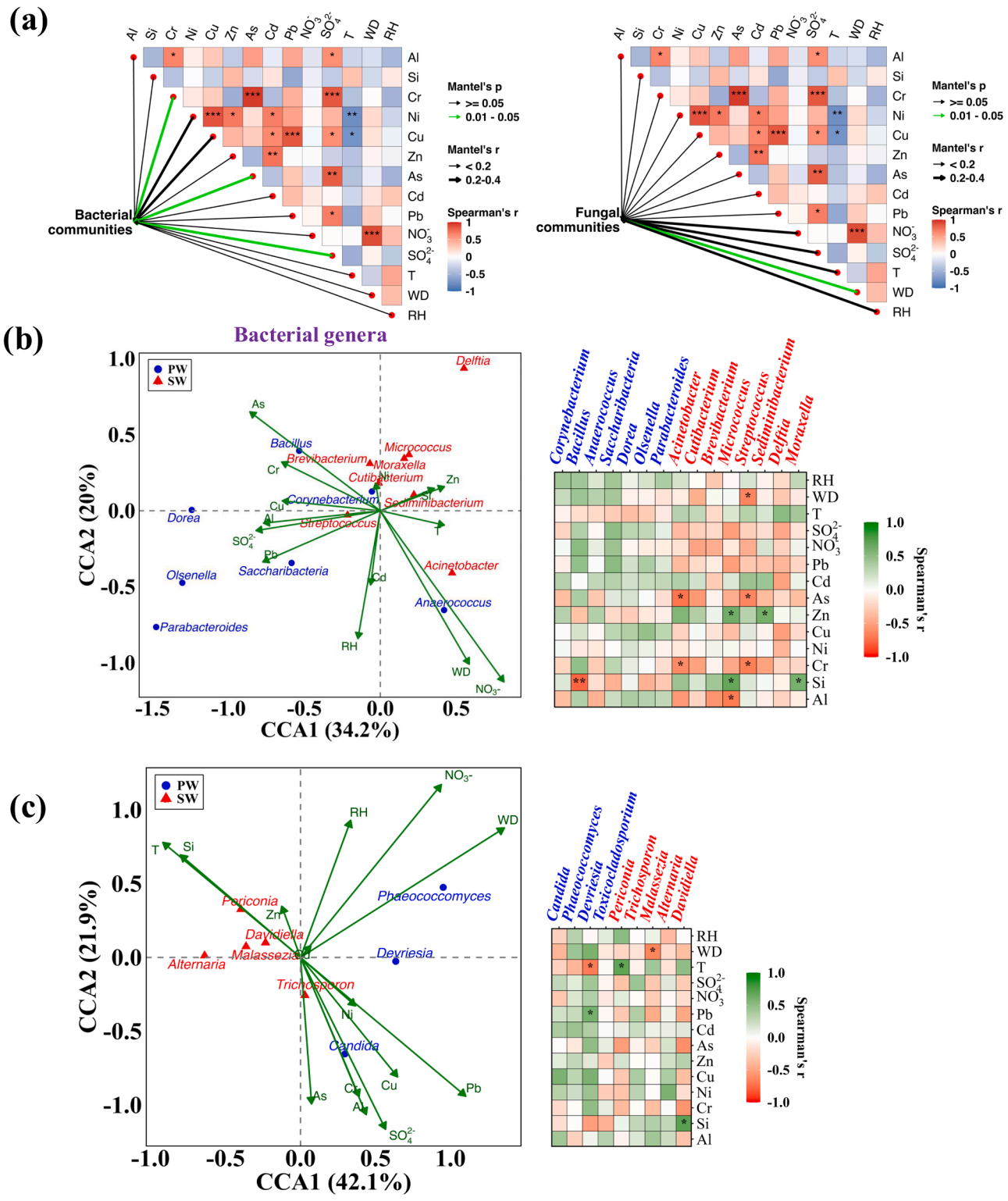

Fig. 7. (a) Mantel test showing influence of environmental variables and meteorological parameters on overall bacterial and fungal communities, (b-c) Canonical Correspondence Analysis (CCA) and Spearman's correlations showing the relationship between individual environmental variables and enriched bacterial and fungal genera in PW and SW. Genera enriched in PW and SW are marked with blue and red colours. Colour scale in the correlation plot represents the strength and direction of the correlation, and asterisks in the plot denote statistical significance (* represents $p < 0.005$, ** represents $p < 0.01$).

Micrococcus. In contrast, toxic metals such As and Cr linked to industrial sources exhibit a significant negative correlation with *Acinetobacter* and *Streptococcus.* Among the meteorological parameters, only WD shows a negative correlation with *Streptococcus,* suggesting that a shift from southerly to northerly wind may suppress bacteria associated with continental sources due to poor adaptability to polar cold conditions.

For fungal communities, CCA reveals that genera such as *Periconia, Davidiella, Malassezia, and Alternaria,* which are enriched under SW regimes, are positively correlated with Zn, Si, and T. Spearman correlation analysis confirms a significant positive correlation of *Davidiella* with Si

and *Periconia* with T, while *Malassezia* exhibits a significant negative correlation with WD. Among the genera enriched under PW conditions, *Devriesia* exhibits a significant negative correlation with T and a significant positive correlation with Pb, emitted from industrial sources. These significant correlations, particularly with toxic metals like Cd and Pb, highlights the metal resistance capability of certain fungal genera (Deng et al., 2025). Overall, the correlation between specific bacterial and fungal genera indicates niche specialisation in response to environmental stresses. Importantly, heavy metals, mainly from urban traffic and industrial emissions from the Eurasia regions, appear to play a key role in shaping the composition of the Arctic microbial community.

4.6. Unveiling microbial co-occurrence through network analysis

Microbes co-exist in the atmosphere, forming complex networks through direct and indirect interactions (Biere and Tack, 2013; Wang et al., 2024). Network analysis can reveal non-random patterns of genus coexistence in microorganisms and also helps to improve the present understanding of the mechanisms that build microbial communities and identify the key genera in the airborne community. In the present study, the co-occurrence network of 20 dominant bacterial and fungal genera in the Arctic air is constructed to elucidate the complex microbial interactions, and the genera are clustered into different categories based on Spearman correlation ($r > 0.6, p > 0.05$) with genus abundance data, as shown in Fig. 8. A total of 29 nodes and 126 edges are identified in this network. Nodes represent individual microbial genera, while edges represent significant associations. Several genera are identified as potential hub species due to their high degree of connectivity within the network. Among them, the bacterium *Methylobacterium* exhibits numerous interactions, including positive associations with *Spirosoma, Duncaniella, Hymenobacter, Sphingomonas*, and *Paramuribaculum*, suggesting their mutualistic relationships within the bacterial community. Similarly, *Sphingomonas* demonstrates both positive (*Methylobacterium, Paramuribaculum, Hymenobacter, Deinococcus*, and *Spirosoma*) and negative (*Acinetobacter, Staphylococcus*, and *Micrococcus*) interactions, underscoring its multifaceted role within the network. Within the bacterial community, *Pseudomonas* forms positive links with *Micrococcus*, which shares certain ecological niches or metabolic capabilities. However, *Pseudomonas* is negatively associated with *Duncanella, Paramuribaculum, Methylobacterium*, and *Sphingomonas*, suggesting competitive dynamics. Notably, significant inter-kingdom associations between bacterial and fungal genera are also observed. *Methylobacterium* shows negative associations with both bacterial genera (*Staphylococcus, Micrococcus*, and *Pseudomonas*) and fungal genera (*Aspergillus, Pleospora,* and *Periconia*), suggesting possible competitive interactions. Fungal genus *Penicillium* shows a negative association with the bacterium *Geobacillus*, potentially indicating competitive exclusion. In contrast, the fungus *Periconia* displays positive associations with certain bacteria, such as *Paramuribaculum*, suggesting potential co-occurrence. Among fungi, *Aspergillus* is positively associated with fungal genus *Davidiella* while negatively associated with bacterial genera such as *Spirosoma* and *Methylobacterium,* suggesting potential antagonism between these genera. These network patterns provide insights into the ecological strategies employed by different microbial taxa. Negative associations may reflect competitive exclusion for limited resources, allelopathy, or differences in preferred environmental conditions. Positive associations, on the other hand, could indicate shared resource utilisation, mutualistic interactions, or a dependency on similar environmental factors. Understanding these specific interactions is crucial for predicting community stability, resilience, and functional capabilities in the Arctic atmosphere. It is important to note that co-occurrence does not necessarily imply direct interaction; rather, it indicates statistical correlation. Further experimental validation would be required to confirm the mechanistic basis of these observed associations.

4.7. Health implications

In the present study, several potential human pathogenic bacterial and fungal genera are identified in wintertime Arctic atmosphere. The principle for identifying pathogenic bacterial and fungal genera is based

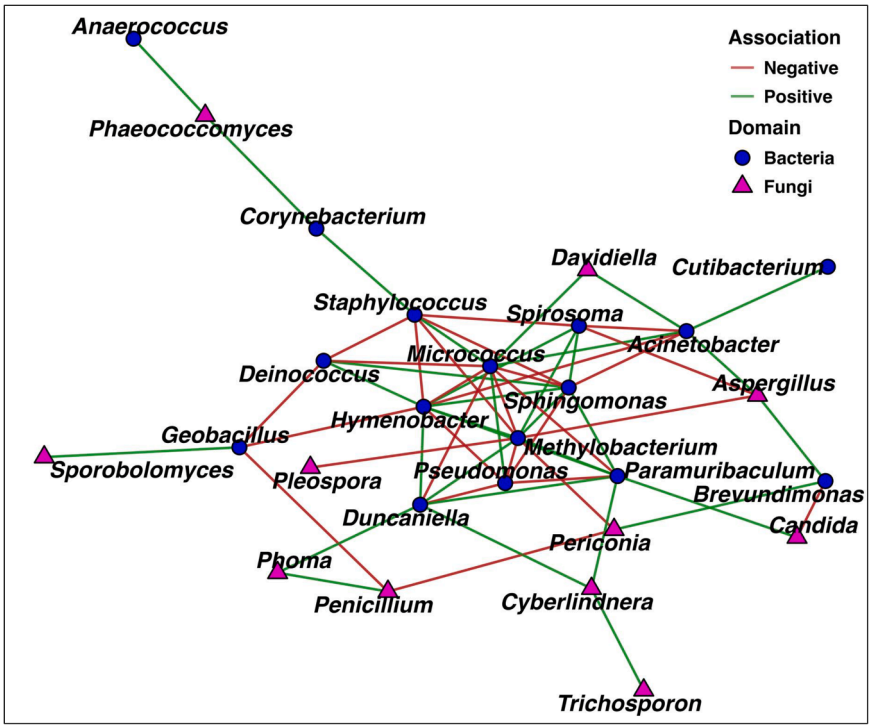

Fig. 8. Co-occurrence network of twenty dominant bacterial and fungal genera present in the Arctic atmosphere. Nodes represent individual genera, coloured by domain (blue: Bacteria; pink: Fungi). Edges represent significant statistical associations between genera. Green edges indicate positive associations. Red edges indicate negative associations.

on recognized pathogenic databases (GlobalRPH; NCBI; Pathogens) and several published literatures (Wang et al., 2024). Fig. 9 (a) illustrates the mean abundance of total genus and pathogenic genus during PW, SW and AP. Notably, bacteria (82) exhibit nearly three times as many potential pathogenic genera as pathogenic fungi (28), highlighting a broader bacterial pathogen spectrum in Arctic air. Interestingly, pathogenic bacterial genera are dominant in PW (49), followed by SW (33) and AP (20). In contrast, pathogenic fungal genera are dominant in AP (20), followed by PW (15) and SW (13). Quantitatively, PW carries 1.5 times more potential pathogenic bacterial genera than SW and more than twice as many as in AP. Conversely, AP carries 1.5 times more pathogenic fungal genera than both PW and SW, respectively. These findings suggest that the PW acts as a major carrier of pathogenic bacteria, whereas AP serves as a more efficient vector for the transport of pathogenic fungi across the Arctic atmosphere. Detailed information on the potential pathogenic bacterial and fungal genera identified in the wintertime Arctic atmosphere is presented in Table 4.

Among bacteria, potential pathogenic genera such as *Acinetobacter*, *Corynebacterium*, and *Staphylococcus* dominate in both PW and SW, while *Pseudomonas* is consistently abundant across all atmospheric conditions, with its maximum abundance in AP (10.8 %). Other notable pathogenic bacterial genera include *Micrococcus, Anaerococcus, Brevibacterium*, and *Cutibacterium* in PW and SW, whereas *Brevundimonas, Massilia, Sphingomonas, Flavobacterium*, and *Nocardiodes* are more prominent in AP. Among fungi, potential pathogenic fungal genera such as *Aspergillus* and *Penicillium* are dominant across all atmospheric conditions, with slightly higher relative abundances in SW. *Candida* and *Phaeococcomyces* are more characteristic of PW, while *Periconia* and *Trichosporon* are enriched in SW. In AP, *Cryptococcus* and *Rhodotorula* are identified as potential pathogenic fungal genera.

In the present study, pathogenic genera are categorised by their target organs in humans and are shown in Fig. 9(b) It is noticed that bacterial genera are more responsible for human infections than fungal genera. Analysis reveals that pathogenic bacterial genera present in the Arctic atmosphere are mostly responsible for bloodstream, gastrointestinal tract (GIT), and skin infections, while fungal pathogenic genera are mainly responsible for respiratory and skin infections. Bloodstream, GIT, oral, and skin infections are more prone to pathogenic bacterial genera present in PW, while respiratory diseases are dominant in SW. The detection of pathogenic bacterial and fungal genera highlights the potential health risks posed by airborne microbial communities, especially in the pristine atmosphere over the Arctic. Present findings highlight the importance of further investigation on species-level identification, virulence gene profiling, and environmental monitoring to assess health implications over the pristine polar region.

5. Summary

Present study investigates atmospheric transport of airborne microbial loading in winter-time Arctic atmosphere, revealing a strong co-occurrence network between bacteria and fungi. A lower cell concentration of $1.5 \pm 0.5 \times 10^4$ cells/m^3 is noticed during winter season in the Arctic atmosphere. However, a significant variation in cell concentration from 0.7×10^4 cells/m^3 to 2.2×10^4 cells/m^3 is observed during wintertime due to shift in wind direction from southerly (SW) to northerly wind (PW).

A 4-fold increase in unique bacterial populations is observed during PW as compared to SW due to the poor adaptability of the continental bacterial population to the harsh, cold polar atmosphere. Present study reveals that airborne microbial community differs significantly from that in precipitation (AP). Interestingly, maximum contribution of the unique bacterial population occurs during precipitation events, suggesting that clouds play a significant role in transporting bacterial community into the Arctic atmosphere. Dominant microorganisms observed during PW and AP are reported to be cold-tolerant.

Arctic airborne fungal diversity exhibits an inverse trend, with comparatively low abundance and lower diversity, reflecting the limited adaptability of fungi in the extreme cold Arctic atmosphere. To examine the relationship between microbial communities and aerosol, present study investigates the chemical composition of the Arctic aerosols and identifies their probable sources. SO_4^{2-} and Zn are the most dominant aerosol types present in the Arctic atmosphere. The source apportion-

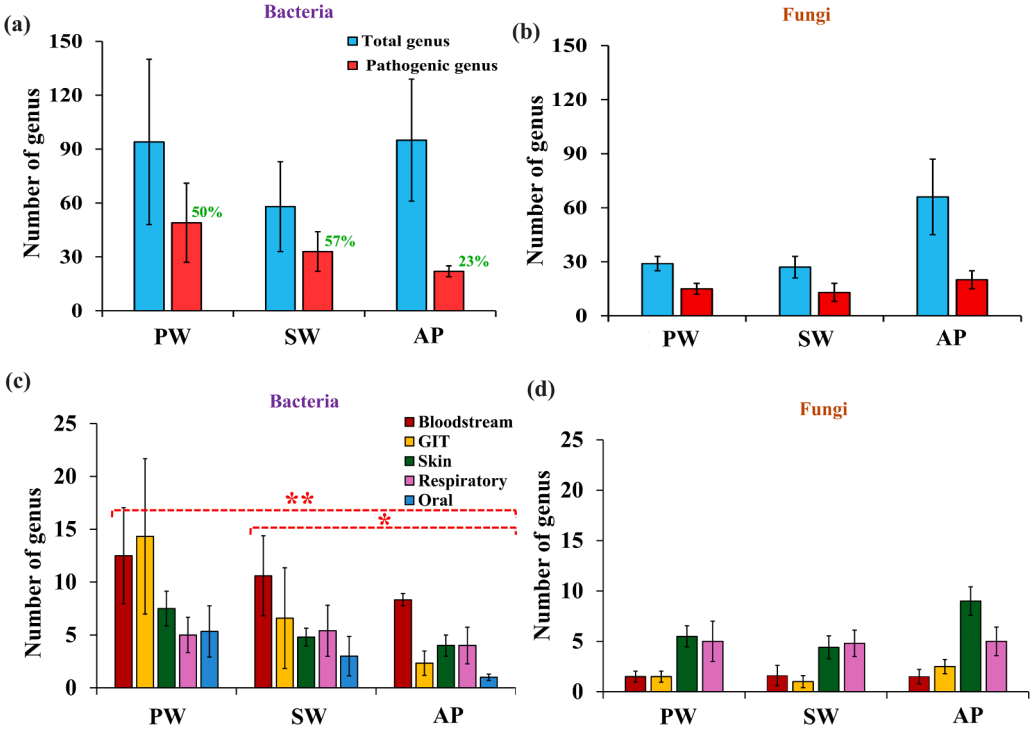

Fig. 9. (a-b) Total genus and pathogenic bacterial and fungal genus identified in PW, SW, and AP, (c-d) Target sites of the pathogenic bacterial and fungal genus in humans.

Table 4
Potential pathogenic bacterial and fungal genera with their relative abundance (%) across different sampling categories in the Arctic atmosphere. Only genera with a relative abundance > 3 % are shown here.

Category	Pathogenic bacterial genera		Pathogenic fungal genera	
	Genus	Abundance (%)	Genus	Abundance (%)
Polar Influenced Northerly Wind (PW)	*Acinetobacter*	12.8	*Aspergillus*	7.1
	Corynebacterium	6.3	*Penicillium*	6.7
	Staphylococcus	6.2	*Candida*	4.5
	Segatella	5.1	*Phaecoccomyces*	3.6
	Mitsuokella	4.6	*Cyberlindnera*	3.0
	Micrococcus	4.5	-	-
	Anaerococcus	4.4	-	-
	Pseudomonas	3.9	-	-
	Haematomicrobium	3.9	-	-
	Cloacibacterium	3.7	-	-
	Brevibacterium	3.3	-	-
	Alistipes	3.2	-	-
	Bacillus	3.0	-	-
	Brevundimonas	3.0	-	-
	Cutibacterium	3.0	-	-
Southerly Wind (SW)	*Acinetobacter*	8.2	*Aspergillus*	7.5
	Corynebacterium	7.1	*Penicillium*	6.1
	Pseudomonas	4.7	*Periconia*	6.1
	Anaerococcus	4.5	*Trichosporon*	3.8
	Methylobacterium	4.5	-	-
	Staphylococcus	4.2	-	-
	Brevibacterium	3.9	-	-
	Streptococcus	3.9	-	-
	Cutibacterium	3.6	-	-
	Massilia	3.5	-	-
	Sediminibacterium	3.5	-	-
	Micrococcus	3.2	-	-
	Delftia	3.0	-	-
Precipitation (AP)	*Pseudomonas*	10.8	*Aspergillus*	6.1
	Brevundimonas	9.0	*Penicillium*	6.1
	Massilia	4.5	*Cryptococcus_1*	4.7
	Sphingomonas	4.5	*Rhodotorula*	3.2
	Flavobacterium	4.2	-	-
	Nocardioides	3.2	-	-

ment analysis suggests that Arctic aerosols originate predominantly from long-range industrial, traffic, and shipping activities. These anthropogenic emissions contain several major ions and metals that significantly influence Arctic airborne bacterial communities.

Present study also identifies several potential human-pathogenic bacterial and fungal genera, with PW and AP serving as carriers of these potential pathogens in the Arctic atmosphere. These findings have important implications, as rapid climate change in the Arctic is noticed in increasing temperatures, resulting in higher potential of cloud availability, and altering Arctic precipitation patterns. Arctic clouds become a potential carrier promoting atmospheric transport of microorganisms, and their subsequent deposition via precipitation, which becomes a potential source of unique microbial inputs to winter-time Arctic atmosphere. Such transported microbial communities can significantly influence regional polar microbial diversity and pathogenic potential, thereby increasing the possible risk to polar human health. The presence of potential pathogenic microorganisms is of particular concern for researchers and personnel operating in remote Arctic regions, where medical infrastructure is limited, and any localised exposure or outbreak could pose serious health consequences. Therefore, understanding potential health impacts is essential for risk assessment, better policy, and management planning in the Arctic region.

Data availability

DNA sequence data for the 16S rRNA and ITS regions generated during the present study have been deposited in the Sequence Read Archive at NCBI-NIH, USA, under BioProject accession numbers PRJNA1338981 and PRJNA1342686.

CRediT authorship contribution statement

Md Abu Mushtaque: Writing – original draft, Visualization, Software, Methodology, Investigation, Formal analysis, Data curation. **Damodararao Karri:** Formal analysis. **Shuvashree Maity:** Formal analysis. **Naveen Gandhi:** Visualization, Formal analysis. **Rohit Srivastava:** Formal analysis. **Christoph Ritter:** Visualization, Formal analysis. **Marion Maturilli:** Visualization, Formal analysis. **Uma Das:** Visualization, Supervision, Formal analysis. **Sanat Kumar Das:** Writing – review & editing, Visualization, Validation, Supervision, Resources, Project administration, Investigation, Funding acquisition, Formal analysis, Conceptualization.

Declaration of competing interest

The authors declare the following financial interests/personal relationships which may be considered as potential competing interests:

Sanat Kumar Das reports financial support, administrative support, article publishing charges, and equipment, drugs, or supplies were provided by Bose Institute. Sanat Kumar Das reports equipment, drugs, or supplies and travel were provided by National Centre for Polar and Ocean Research. Reports a relationship with that includes:. Has patent pending to. If there are other authors, they declare that they have no known competing financial interests or personal relationships that could have appeared to influence the work reported in this paper.

Acknowledgments

Authors are thankful to the Director, Bose Institute for providing financial support to conduct this research. Authors would like to thank

the National Centre for Polar and Ocean Research (NCPOR), Ministry of Earth Science (MOES) GoI, for logistical support to collect samples at Ny-Ålesund. Discussions with Prof. Gyana Ranjan Tripathy (IISER Pune) were helpful during this study. The authors would like to thank the University Grants Commission (UGC), GoI, for providing a fellowship. Authors would also like to extend their acknowledgements to the National Oceanic and Atmospheric Administration (NOAA) and Air Resource Laboratory (ARL) for providing HySPLIT model data and AWI for meteorology and lidar data.

Supplementary materials

Supplementary material associated with this article can be found, in the online version, at doi:10.1016/j.temicr.2026.100070.

References

Achtert, P., O'Connor, E.J., Brooks, I.M., Sotiropoulou, G., Shupe, M.D., Pospichal, B., Brooks, B.J., Tjernström, M., 2020. Properties of Arctic liquid and mixed-phase clouds from shipborne Cloudnet observations during ACSE 2014. Atmos. Chem. Phys. 20, 14983–15002. https://doi.org/10.5194/acp-20-14983-2020.

Adamiec, E., Jarosz-Krzemińska, E., Wieszała, R., 2016. Heavy metals from non-exhaust vehicle emissions in urban and motorway road dusts. Environ. Monit. Assess. 188, 369. https://doi.org/10.1007/s10661-016-5377-1.

Altıkulaç, A., Turhan, Ş., Kurnaz, A., Gören, E., Duran, C., Hançerlioğulları, A., Uğur, F. A., 2022. Assessment of the enrichment of heavy metals in coal and its combustion residues. ACS. Omega 7, 21239–21245. https://doi.org/10.1021/acsomega.2c02308.

Amato, P., Joly, M., Besaury, L., Oudart, A., Taib, N., Moné, A.I., Deguillaume, L., Delort, A.-M., Debroas, D., 2017. Active microorganisms thrive among extremely diverse communities in cloud water. PLoS. One 12, e0182869. https://doi.org/10.1371/journal.pone.0182869.

Amato, P., Ménager, M., Sancelme, M., Laj, P., Mailhot, G., Delort, A.-M., 2005. Microbial population in cloud water at the Puy de Dôme: implications for the chemistry of clouds. Atmos. Environ. 39, 4143–4153. https://doi.org/10.1016/j.atmosenv.2005.04.002.

Bauer, H., Giebl, H., Hitzenberger, R., Kasper-Giebl, A., Reischl, G., Zibuschka, F., Puxbaum, H., 2003. Airborne bacteria as cloud condensation nuclei. J. Geophys. Res. 108, 2003JD003545. https://doi.org/10.1029/2003JD003545.

Biere, A., Tack, A.J.M., 2013. Evolutionary adaptation in three-way interactions between plants, microbes and arthropods. Funct. Ecol. 27, 646–660. https://doi.org/10.1111/1365-2435.12096.

Blagojević, J., Vukojević, J., Ivanović, B., Ivanović, Ž., 2020. Characterization of *alternaria* species associated with leaf spot disease of *armoracia rusticana* in Serbia. Plant Dis. 104, 1378–1389. https://doi.org/10.1094/PDIS-02-19-0289-RE.

Bokhorst, S., Pedersen, S.H., Brucker, L., Anisimov, O., Bjerke, J.W., Brown, R.D., Ehrich, D., Essery, R.L.H., Heilig, A., Ingvander, S., Johansson, C., Johansson, M., Jónsdóttir, I.S., Inga, N., Luojus, K., Macelloni, G., Mariash, H., McLennan, D., Rosqvist, G.N., Sato, A., Savela, H., Schneebeli, M., Sokolov, A., Sokratov, S.A., Terzago, S., Vikhamar-Schuler, D., Williamson, S., Qiu, Y., Callaghan, T.V., 2016. Changing Arctic snow cover: A review of recent developments and assessment of future needs for observations, modelling, and impacts. Ambio 45, 516–537. https://doi.org/10.1007/s13280-016-0770-0.

Bozem, H., Hoor, P., Kunkel, D., Köllner, F., Schneider, J., Herber, A., Schulz, H., Leaitch, W.R., Aliabadi, A.A., Willis, M.D., Burkart, J., Abbatt, J.P.D., 2019. Characterization of transport regimes and the polar dome during arctic spring and summer using in situ aircraft measurements. Atmos. Chem. Phys. 19, 15049–15071. https://doi.org/10.5194/acp-19-15049-2019.

Brągoszewska, E., Pastuszka, J.S., 2018. Influence of meteorological factors on the level and characteristics of culturable bacteria in the air in Gliwice, Upper Silesia (Poland). Aerobio. (Bologna) 34, 241–255. https://doi.org/10.1007/s10453-018-9510-1.

Butinar, L., Spencer-Martins, I., Gunde-Cimerman, N., 2007. Yeasts in high Arctic glaciers: the discovery of a new habitat for eukaryotic microorganisms. Antonie Leeuwenhoek 91, 277–289. https://doi.org/10.1007/s10482-006-9117-3.

Cao, Y., Yu, X., Ju, F., Zhan, H., Jiang, B., Kang, H., Xie, Z., 2021. Airborne bacterial community diversity, source and function along the Antarctic Coast. Sci. Total Environ. 765, 142700. https://doi.org/10.1016/j.scitotenv.2020.142700.

Cavicchioli, R., Ripple, W.J., Timmis, K.N., Azam, F., Bakken, L.R., Baylis, M., Behrenfeld, M.J., Boetius, A., Boyd, P.W., Classen, A.T., Crowther, T.W., Danovaro, R., Foreman, C.M., Huisman, J., Hutchins, D.A., Jansson, J.K., Karl, D.M., Koskella, B., Mark Welch, D.B., Martiny, J.B.H., Moran, M.A., Orphan, V.J., Reay, D. S., Remais, J.V., Rich, V.I., Singh, B.K., Stein, L.Y., Stewart, F.J., Sullivan, M.B., Van Oppen, M.J.H., Weaver, S.C., Webb, E.A., Webster, N.S., 2019. Scientists' warning to humanity: microorganisms and climate change. Nat. Rev. Microbiol. 17, 569–586. https://doi.org/10.1038/s41579-019-0222-5.

Chen, Y., Shi, Z.W., Strickland, A.B., Shi, M., 2022. Cryptococcus neoformans infection in the Central Nervous system: the battle between host and pathogen. JoF 8, 1069. https://doi.org/10.3390/jof8101069.

Cho, Y., Park, S.-J., Kim, J.-H., Yeo, H., Nam, J., Jun, S.-Y., Kim, B.-M., Kim, S.-W., 2021. Investigating wintertime cloud microphysical properties and their relationship to air mass advection at Ny-Ålesund, Svalbard using the synergy of a cloud radar–Ceilometer–Microwave radiometer. Remote Sens. (Basel) 13, 2529. https://doi.org/10.3390/rs13132529.

Cody, Y.S., Gross, D.C., 1987. Characterization of Pyoverdin$_{pss}$, the fluorescent siderophore produced by *Pseudomonas syringae* pv. *syringae*. Appl. Environ. Microbiol. 53, 928–934. https://doi.org/10.1128/aem.53.5.928-934.1987.

Coutinho, M.L., Miller, A.Z., Phillip, A., Mirão, J., Dias, L., Rogerio-Candelera, M.A., Saiz-Jimenez, C., Martin-Sanchez, P.M., Cerqueira-Alves, L., Macedo, M.F., 2019. Biodeterioration of majolica glazed tiles by the fungus Devriesia imbrexigena. Constr. Build. Mater. 212, 49–56. https://doi.org/10.1016/j.conbuildmat.2019.03.268.

Deng, J., Wang, Y., Yu, D., Li, X., Yue, J., 2025. Effects of heavy metals on variation in bacterial communities in farmland soil of tailing dam collapse area. Sci. Rep. 15, 8100. https://doi.org/10.1038/s41598-025-93244-6.

Després, V.R., Huffman, J.A., Burrows, S.M., Hoose, C., Safatov, A.S., Buryak, G., Fröhlich-Nowoisky, J., Elbert, W., Andreae, M.O., Pöschl, U., Jaenicke, R., 2012. Primary biological aerosol particles in the atmosphere: A review. Tellus B: Chem. Phys. Meteorol. 64, 15598. https://doi.org/10.3402/tellusb.v64i0.15598.

Dijkshoorn, L., Nemec, A., Seifert, H., 2007. An increasing threat in hospitals: multidrug-resistant Acinetobacter baumannii. Nat. Rev. Microbiol. 5, 939–951. https://doi.org/10.1038/nrmicro1789.

Doytchinov, V.V., Dimov, S.G., 2022. Microbial community composition of the antarctic ecosystems: review of the bacteria, fungi, and archaea identified through an NGS-based metagenomics approach. Life 12, 916. https://doi.org/10.3390/life12060916.

Dvoretsky, V.G., Venger, M.P., Vashchenko, A.V., Maksimovskaya, T.M., Ishkulova, T.G., Vodopianova, V.V., 2022. Pelagic bacteria and viruses in a high arctic region: environmental control in the autumn period. Biology. (Basel) 11, 845. https://doi.org/10.3390/biology11060845.

Eiler, A., Langenheder, S., Bertilsson, S., Tranvik, L.J., 2003. Heterotrophic bacterial growth efficiency and community structure at different natural organic carbon concentrations. Appl. Environ. Microbiol. 69, 3701–3709. https://doi.org/10.1128/AEM.69.7.3701-3709.2003.

Elkhapery, A., Fatima, M., Soubani, A.O., 2025. Emerging risk factors for invasive pulmonary aspergillosis: A narrative review. JoF 11, 555. https://doi.org/10.3390/jof11080555.

Francis, J., Skific, N., 2015. Evidence linking rapid Arctic warming to mid-latitude weather patterns. Philos. Trans. a Math. Phys. Eng. Sci. 373, 20140170. https://doi.org/10.1098/rsta.2014.0170.

Fröhlich-Nowoisky, J., Kampf, C.J., Weber, B., Huffman, J.A., Pöhlker, C., Andreae, M. O., Lang-Yona, N., Burrows, S.M., Gunthe, S.S., Elbert, W., Su, H., Hoor, P., Thines, E., Hoffmann, T., Després, V.R., Pöschl, U., 2016. Bioaerosols in the Earth system: climate, health, and ecosystem interactions. Atmos. Res. 182, 346–376. https://doi.org/10.1016/j.atmosres.2016.07.018.

Fuzzi, S., Mandrioli, P., Perfetto, A., 1997. Fog droplets—An atmospheric source of secondary biological aerosol particles. Atmos. Environ. 31, 287–290. https://doi.org/10.1016/1352-2310(96)00160-4.

Gaitanis, G., Magiatis, P., Hantschke, M., Bassukas, I.D., Velegraki, A., 2012. The Malassezia genus in skin and systemic diseases. Clin. Microbiol. Rev. 25, 106–141. https://doi.org/10.1128/CMR.00021-11.

Gherardi, G., 2023. Staphylococcus aureus infection: pathogenesis and antimicrobial resistance. IJMS 24, 8182. https://doi.org/10.3390/ijms24098182.

GlobalRPH, https://globalrph.com/bacteria.

Harding, T., Jungblut, A.D., Lovejoy, C., Vincent, W.F., 2011. Microbes in high arctic snow and implications for the cold biosphere. Appl. Environ. Microbiol. 77, 3234–3243. https://doi.org/10.1128/AEM.02611-10.

Hawari, A., Qasem, M., Alhajyaseen, W., 2021. Concentration of Pb, Cu, Zn and Cdin the roadside soil of Doha: effect of TrafficVolume and season. Pol. J. Environ. Stud. 30, 3579–3586. https://doi.org/10.15244/pjoes/127387.

Herrmann, H., 2003. Kinetics of aqueous phase reactions relevant for atmospheric chemistry. Chem. Rev. 103, 4691–4716. https://doi.org/10.1021/cr020658q.

Hopwood, M.J., Carroll, D., Dunse, T., Hodson, A., Holding, J.M., Iriarte, J.L., Ribeiro, S., Achterberg, E.P., Cantoni, C., Carlson, D.F., Chierici, M., Clarke, J.S., Cozzi, S., Fransson, A., Juul-Pedersen, T., Winding, M.H.S., Meire, L., 2020. Review article: how does glacier discharge affect marine biogeochemistry and primary production in the Arctic? Cryosphere 14, 1347–1383. https://doi.org/10.5194/tc-14-1347-2020.

Huang, X., Hu, J., Qin, F., Quan, W., Cao, R., Fan, M., Wu, X., 2017. Heavy metal pollution and ecological assessment around the Jinsha coal-fired Power plant (China). Int. J. Environ. Res. Public Health 14, 1589. https://doi.org/10.3390/ijerph14121589.

Jarrige, D., Haridas, S., Bleykasten-Grosshans, C., Joly, M., Nadalig, T., Sancelme, M., Vuilleumier, S., Grigoriev, I.V., Amato, P., Bringel, F., 2022. High-quality genome of the basidiomycete yeast dioszegia hungarica PDD-24b-2 isolated from cloud water. G3. (Bethesda) 12, jkac282. https://doi.org/10.1093/g3journal/jkac282.

Jensen, L.Z., Glasius, M., Gryning, S.-E., Massling, A., Finster, K., Šantl-Temkiv, T., 2022. Seasonal variation of the atmospheric bacterial community in the Greenlandic high Arctic is influenced by weather events and local and distant sources. Front. Microbiol. 13, 909980. https://doi.org/10.3389/fmicb.2022.909980.

John, H.T., Thomas, T.C., Chukwuebuka, E.C., Ali, A.B., Anass, R., Tefera, Y.Y., Babu, B., Negrut, N., Ferician, A., Marian, P., 2025. The microbiota-Human health axis. Microorganisms 13, 948. https://doi.org/10.3390/microorganisms13040948.

Kourtev, P.S., Hill, K.A., Shepson, P.B., Konopka, A., 2011. Atmospheric cloud water contains a diverse bacterial community. Atmos. Environ. 45, 5399–5405. https://doi.org/10.1016/j.atmosenv.2011.06.041.

Labus, K., 1995. Heavy-metal emissions from coal combustion in Southwestern Poland. Energy 20, 1115–1119. https://doi.org/10.1016/0360-5442(95)00062-L.

Lange, R., Dall'Osto, M., Wex, H., Skov, H., Massling, A., 2019. Large summer contribution of organic biogenic aerosols to arctic cloud condensation nuclei. Geophys. Res. Lett. 46, 11500–11509. https://doi.org/10.1029/2019GL084142.
Lenton, T.M., Held, H., Kriegler, E., Hall, J.W., Lucht, W., Rahmstorf, S., Schellnhuber, H. J., 2008. Tipping elements in the Earth's climate system. Proc. Natl. Acad. Sci. U.S.A. 105, 1786–1793. https://doi.org/10.1073/pnas.0705414105.
Loughran, A.J., Orihuela, C.J., Tuomanen, E.I., 2019. *Streptococcus pneumoniae* : invasion and inflammation. Microbiol. Spectr. 7, 15. https://doi.org/10.1128/microbiolspec.GPP3-0004-2018, 7.2.
Makled, A.F., Ali, S.A.M., Labeeb, A.Z., Salman, S.S., Shebl, D.Z.M., Hegazy, S.G., Sabal, M.S., 2024. Characterization of Candida species isolated from clinical specimens: insights into virulence traits, antifungal resistance and molecular profiles. BMC. Microbiol. 24, 388. https://doi.org/10.1186/s12866-024-03515-x.
Malard, L.A., Avila-Jimenez, M.-L., Schmale, J., Cuthbertson, L., Cockerton, L., Pearce, D. A., 2022. Aerobiology over the Southern Ocean – Implications for bacterial colonization of Antarctica. Environ. Int. 169, 107492. https://doi.org/10.1016/j.envint.2022.107492.
Malard, L.A., Bergk-Pinto, B., Layton, R., Vogel, T.M., Larose, C., Pearce, D.A., 2023. Snow microorganisms colonise arctic soils following Snow melt. Microb. Ecol. 86, 1661–1675. https://doi.org/10.1007/s00248-023-02204-y.
Margesin, R., Fonteyne, P.-A., Schinner, F., Sampaio, J.P., 2007. Rhodotorula psychrophila sp. nov., Rhodotorula psychrophenolica sp. nov. And Rhodotorula glacialis sp. nov., novel psychrophilic basidiomycetous yeast species isolated from alpine environments. Int. J. Syst. Evol. Microbiol. 57, 2179–2184. https://doi.org/10.1099/ijs.0.65111-0.
Maturilli, M., Herber, A., König-Langlo, G., 2013. Continuous meteorological observations at station Ny-Ålesund, 1993-08 to 2011-07. https://doi.org/10.1594/PANGAEA.793046.
Mayslich, C., Grange, P.A., Dupin, N., 2021. Cutibacterium acnes as an opportunistic pathogen: an update of its virulence-associated factors. Microorganisms. 9, 303. https://doi.org/10.3390/microorganisms9020303.
Mirzabeygi, M., Abbasnia, A., Yunesian, M., Nodehi, R.N., Yousefi, N., Hadi, M., Mahvi, A.H., 2017. Heavy metal contamination and health risk assessment in drinking water of Sistan and Baluchistan, Southeastern Iran. Hum. Ecol. Risk Assess.: Int. J. 23, 1893–1905. https://doi.org/10.1080/10807039.2017.1322895.
Munawer, M.E., 2018. Human health and environmental impacts of coal combustion and post-combustion wastes. J. Sustain. Min. 17, 87–96. https://doi.org/10.1016/j.jsm.2017.12.007.
Mushtaque, M.A., Saikh, S.R., Biswas, A., Darbha, G.K., Das, S.K., 2025. Source-specific multi-pathway human health risk assessment of metals present in clouds over Indian Subcontinent. Environ. Adv. 21, 100647. https://doi.org/10.1016/j.envadv.2025.100647.
NCBI, (https://www.ncbi.nlm.nih.gov/pathogens/organisms).
Nemec, A., De Baere, T., Tjernberg, I., Vaneechoutte, M., Van Der Reijden, T.J., Dijkshoorn, L., 2001. Acinetobacter ursingii sp. nov. And Acinetobacter schindleri sp. nov., isolated from human clinical specimens. Int. J. Syst. Evol. Microbiol. 51, 1891–1899. https://doi.org/10.1099/00207713-51-5-1891.
Nemec, A., Radolfova-Krizova, L., 2016. Acinetobacter pakistanensis Abbas et al. 2014 is a later heterotypic synonym of Acinetobacter bohemicus Krizova et al. 2014. Int. J. Syst. Evol. Microbiol. 66, 5614–5617. https://doi.org/10.1099/ijsem.0.001530.
Pathogens, https://www.pathogensportal.org/pathogen-classifications.
Péguilhan, R., Rossi, F., Rué, O., Joly, M., Amato, P., 2023. Comparative analysis of bacterial diversity in clouds and aerosols. Atmos. Environ. 298, 119635. https://doi.org/10.1016/j.atmosenv.2023.119635.
Pramanick, A., Saikh, S.R., Mushtaque, Md.A., Karri, D., Gandhi, N., Das, S.K., 2025. Long-range transported bacteria perturbing airborne bacterial diversity and pathogenicity over Eastern Himalayas, India. Sci. Total Environ. 1008, 180981. https://doi.org/10.1016/j.scitotenv.2025.180981.
Rantanen, M., Karpechko, A.Yu., Lipponen, A., Nordling, K., Hyvärinen, O., Ruosteenoja, K., Vihma, T., Laaksonen, A., 2022. The Arctic has warmed nearly four times faster than the globe since 1979. Commun. Earth. Environ. 3, 168. https://doi.org/10.1038/s43247-022-00498-3.
Saikh, S.R., Das, S.K., 2023. Fog-induced alteration in airborne microbial community: A study over Central Indo-Gangetic plain in India. Appl. Environ. Microbiol. 89, e01367. https://doi.org/10.1128/aem.01367-22. -22.
Saikh, S.R., Pramanick, A., Yasutomi, N., Biswal, A., Ghude, S., Sharma, A., Dimri, A.P., Ueda, K., Patra, P.K., Das, S.K., 2025. Population dependent alteration in urban airborne bacterial communities enriched with pathogens: A study over Delhi, India. Atmos. Environ.: X 27, 100351. https://doi.org/10.1016/j.aeaoa.2025.100351.
Šantl-Temkiv, T., Gosewinkel, U., Starnawski, P., Lever, M., Finster, K., 2018. Aeolian dispersal of bacteria in southwest Greenland: their sources, abundance, diversity and physiological states. FEMS. Microbiol. Ecol. 94 (4), fiy031. https://doi.org/10.1093/femsec/fiy031.
Šantl-Temkiv, T., Lange, R., Beddows, D., Rauter, U., Pilgaard, S., Dall'Osto, M., Gunde-Cimerman, N., Massling, A., Wex, H., 2019. Biogenic sources of ice nucleating particles at the high Arctic site Villum Research Station. Environ. Sci. Technol. 53, 10580–10590. https://doi.org/10.1021/acs.est.9b00991.
Sasgen, I., Steinhoefel, G., Kasprzyk, C., Matthes, H., Westermann, S., Boike, J., Grosse, G., 2024. Atmosphere circulation patterns synchronize pan-Arctic glacier melt and permafrost thaw. Commun. Earth. Environ. 5, 375. https://doi.org/10.1038/s43247-024-01548-8.
Schmale, J., Sharma, S., Decesari, S., Pernov, J., Massling, A., Hansson, H.-C., Von Salzen, K., Skov, H., Andrews, E., Quinn, P.K., Upchurch, L.M., Eleftheriadis, K., Traversi, R., Gilardoni, S., Mazzola, M., Laing, J., Hopke, P., 2022. Pan-Arctic seasonal cycles and long-term trends of aerosol properties from 10 observatories. Atmos. Chem. Phys. 22, 3067–3096. https://doi.org/10.5194/acp-22-3067-2022.
Setlow, P., 2006. Spores of Bacillus subtilis: their resistance to and killing by radiation, heat and chemicals. J. Appl. Microbiol. 101, 514–525. https://doi.org/10.1111/j.1365-2672.2005.02736.x.
Shaw, G.E., 1995. The Arctic haze phenomenon. Bull. Amer. Meteor. Soc. 76, 2403–2413. https://doi.org/10.1175/1520-0477(1995)076<2403:TAHP>2.0.CO;2.
Sonbawne, S.M., Raju, M.P., Safai, P.D., Devara, P.C.S., Fadnavis, S., Panicker, A.S., Pandithurai, G., 2023. Size-separated aerosol chemical characterization over Ny-Ålesund during the Arctic summer of 2010. Sustain. Chem. Clim. Action 2, 100016. https://doi.org/10.1016/j.scca.2023.100016.
Sorahan, T., Esmen, N.A., 2004. Lung cancer mortality in UK nickel-cadmium battery workers, 1947–2000. Occup. Environ. Med. 61, 108–116. https://doi.org/10.1136/oem.2003.009282.
Stohl, A., 2006. Characteristics of atmospheric transport into the Arctic troposphere. J. Geophys. Res. 111, 2005JD006888. https://doi.org/10.1029/2005JD006888.
Tignat-Perrier, R., Dommergue, A., Thollot, A., Keuschnig, C., Magand, O., Vogel, T.M., Larose, C., 2019. Global airborne microbial communities controlled by surrounding landscapes and wind conditions. Sci. Rep. 9, 14441. https://doi.org/10.1038/s41598-019-51073-4.
Vaïtilingom, M., Attard, E., Gaiani, N., Sancelme, M., Deguillaume, L., Flossmann, A.I., Amato, P., Delort, A.-M., 2012. Long-term features of cloud microbiology at the puy de Dôme (France). Atmos. Environ. 56, 88–100. https://doi.org/10.1016/j.atmosenv.2012.03.072.
Velsko, I.M., Warinner, C., 2025. Streptococcus abundance and oral site tropism in humans and non-human primates reflects host and lifestyle differences. NPJ. Biofilms. Microbiomes. 11, 19. https://doi.org/10.1038/s41522-024-00642-1.
Vincent, W.F., 2010. Microbial ecosystem responses to rapid climate change in the Arctic. ISMe J. 4, 1087–1090. https://doi.org/10.1038/ismej.2010.108.
Wang, Y., Wang, W., Yu, X., Wang, Z., Zhou, Z., Han, Y., Li, L., 2024. Global diversity of airborne pathogenic bacteria and fungi from wastewater treatment plants. Water. Res. 258, 121764. https://doi.org/10.1016/j.watres.2024.121764.
Wei, M., Xu, C., Chen, J., Zhu, C., Li, J., Lv, G., 2017. Characteristics of bacterial community in cloud water at Mt Tai: similarity and disparity under polluted and non-polluted cloud episodes. Atmos. Chem. Phys. 17, 5253–5270. https://doi.org/10.5194/acp-17-5253-2017.
Zaragoza, O., Rodrigues, M.L., De Jesus, M., Frases, S., Dadachova, E., Casadevall, A., 2009. The capsule of the fungal pathogen Cryptococcus neoformans. Adv. Appl. Microbiol. 68, 133–216. https://doi.org/10.1016/S0065-2164(09)01204-0.
Zhu, C., Chen, J., Wang, X., Li, J., Wei, M., Xu, C., Xu, X., Ding, A., Collett Jr., J.L., 2018. Chemical composition and bacterial community in size-resolved cloud water at the summit of Mt. Tai, China. Aerosol Air Qual. Res. 18, 1–14. https://doi.org/10.4209/aaqr.2016.11.0493.